HAL
open science

Qualitative Simulation of the Initiation of Sporulation in B. subtilis

Hidde De jong, Johannes Geiselmann, Grégory Batt, Céline Hernandez, Michel Page

To cite this version:

Hidde De jong, Johannes Geiselmann, Grégory Batt, Céline Hernandez, Michel Page. Qualitative Simulation of the Initiation of Sporulation in B. subtilis. [Research Report] RR-4527, INRIA. 2002. inria-00072061

HAL Id: inria-00072061

https://inria.hal.science/inria-00072061v1

Submitted on 23 May 2006

HAL is a multi-disciplinary open access archive for the deposit and dissemination of scientific research documents, whether they are published or not. The documents may come from teaching and research institutions in France or abroad, or from public or private research centers.

L'archive ouverte pluridisciplinaire **HAL**, est destinée au dépôt et à la diffusion de documents scientifiques de niveau recherche, publiés ou non, émanant des établissements d'enseignement et de recherche français ou étrangers, des laboratoires publics ou privés.

INSTITUT NATIONAL DE RECHERCHE EN INFORMATIQUE ET EN AUTOMATIQUE

Qualitative Simulation of the Initiation of Sporulation in *B. subtilis*

Hidde de Jong — Johannes Geiselmann — Grégory Batt — Céline Hernandez — Michel Page

N° 4527

Aout 2002

THÈME 3

Rapport de recherche

ISSN 0249-6399 ISRN INRIA/RR--4527--FR+ENG

Qualitative Simulation of the Initiation of Sporulation in *B. subtilis*

Hidde de Jong , Johannes Geiselmann* , Grégory Batt , Céline Hernandez , Michel Page

Thème 3 — Interaction homme-machine,
images, données, connaissances
Projets HELIX

Rapport de recherche n° 4527 — Aout 2002 — 41 pages

Abstract: Under conditions of nutrient deprivation, the Gram positive soil bacterium *Bacillus subtilis* can abandon vegetative growth and form a dormant, environmentally-resistant spore instead. The decision to either divide or sporulate is controlled by a large and complex genetic regulatory network integrating various environmental, cell-cycle, and metabolic signals. Although sporulation in *B. subtilis* is one of the best-understood model systems for prokaryotic development, very little quantitative data on kinetic parameters and molecular concentrations are available. A qualitative simulation method is used to model the sporulation network and simulate the response of the cell to nutrient deprivation. Using this method, we have been able to reproduce essential features of the choice between vegetative growth and sporulation, in particular the role played by competing positive and negative feedback loops.

Key-words: genetic regulatory networks, mathematical modeling, piecewise-linear differential equations, qualitative simulation, mathematical biology, bioinformatics, sporulation, *B. subtilis*

* Laboratoire Plasticité et Expression des Génomes Microbiens, Université Joseph Fourier, Grenoble.

Unité de recherche INRIA Rhône-Alpes
655, avenue de l'Europe, 38330 Montbonnot-St-Martin (France)
Téléphone : +33 4 76 61 52 00 —Télécopie +33 4 76 61 52 52

Simulation qualitative de l'initiation de la sporulation chez *B. subtilis*

Résumé : Dans des conditions de privation de nutriments, la bactérie du sol Gram-positif *Bacillus subtilis* peut abandonner la croissance végétative et former une spore dormante et résistante aux facteurs environnementaux. La décision de se diviser ou bien de sporuler est contrôlée par un grand réseau de régulation génique complexe qui intègre plusieurs signaux environnementaux, signaux du cycle cellulaire et signaux métaboliques. Même si la sporulation chez *B. subtilis* est un des systèmes de modèle le mieux compris, très peu de données quantitatives sur les paramètres cinétiques et les concentrations moléculaires sont disponibles. Une méthode de simulation qualitative est utilisée pour modéliser le réseau de sporulation et pour simuler la réponse de la cellule à la privation de nutriments. En utilisant cette méthode, nous avons été capables de reproduire les caractéristiques essentielles du choix entre la croissance végétative et la sporulation, en particulier le rôle joué par des boucles de rétroaction positives et négatives.

Mots-clés : réseaux de régulation génique, modélisation mathématique, équations différentielles linéaires par morceaux, simulation qualitative, biologie mathématique, bioinformatique, sporulation, *B. subtilis*

1 Introduction

Under conditions of nutrient deprivation, the Gram positive soil bacterium *Bacillus subtilis* initiates a range of responses that allow it to survive in the increasingly hostile environment [28, 32, 64, 72, 75]. Among these responses are the production of antibiotics, the development of motility and competence, and as a final resort, the formation of dormant, environmentally-resistant spores. The decision to abandon vegetative growth and enter sporulation has far-reaching consequences for the bacterium. It involves a switch between two completely different genetic programs entailing energy-expensive changes in gene expression and morphology [5, 28, 35, 76, 77].

The changes in gene expression and morphology induced by sporulation are regulated by a complex regulatory network involving more than 125 genes [17, 77]. The size and complexity of the sporulation network make it difficult to interpret the switch from vegetative growth to sporulation in terms of the interactions between genes, proteins, and small molecules. Computer modeling and simulation may help in understanding how a global response can emerge from a network of local interactions. In addition, the use of modeling and simulation tools may permit the formulation of hypotheses on missing components and interactions which, after a process of screening through computer simulation, can guide further experimentation.

Notwithstanding the enormous amount of work devoted to the elucidation of the network of interactions underlying the sporulation process, very little quantitative data on kinetic parameters and molecular concentrations are available. As a consequence, traditional methods for the numerical analysis and simulation of biochemical systems are difficult to apply. In the accompanying report [10], a method for the qualitative simulation of genetic regulatory networks has been described that does not depend on precise numerical values for the parameters and initial conditions. Rather, it exploits qualitative constraints in the form of parameter inequalities that can usually be inferred from the experimental literature. The method is based on a class of piecewise-linear (PL) differential equation models of genetic regulatory networks that, while abstracting from the precise molecular mechanisms involved, capture essential aspects of gene regulation [25, 54, 74].

In this report, we will apply the qualitative simulation method described in [10] to model the sporulation network and to simulate the response of the cell to nutrient deprivation. The aim is to show that the method is able to reproduce experimental findings in the case of a large and complex network that is well-understood by molecular biologists. In particular, the simulations should clarify how the choice between alternative developmental pathways, sporulation and vegetative growth, emerges from a network of molecular interactions. To our knowledge, except for a previous version of the model presented here [11], no modeling and simulation studies of sporulation in *B. subtilis* have been published thus far.

The model of the regulatory network has been constructed from the extensive literature on sporulation in *B. subtilis* and computerized resources like the database SubtiList [55]. It consists of a dozen differential equations representing the evolution of the concentration of key proteins in the sporulation network, as well as inequalities constraining the parameter values. Using this model, the response of wild type and mutant bacteria to physiological perturbations has been simulated by means of the computer program Genetic Network Analyzer [9], which implements the qualitative simulation method mentioned above. Each simulation results in a graph of qualitative states and transitions between qualitative states, representing all possible qualitative behaviors of the bacterium.

Comparison of the predicted and observed behaviors reveals that essential features of the response of the cell to nutrient deprivation can be reproduced by means of the model. In fact, the qualitative behaviors in the transition graph correspond either to the continuation of vegetative growth or to the initiation of sporulation. Closer analysis shows that the choice between these alternative pathways is determined by competing positive and negative feedback loops influencing the accumulation of the phosphorylated transcription factor Spo0A. If the positive feedback loops favoring phosphorylation of Spo0A outweigh the negative feedback loops favoring dephosphorylation, then Spo0A$\sim$P may reach

a concentration at which it starts to activate genes whose expression commits the cell to sporulation. If this is not the case, the cell continues to grow and divide. The attainment of a critical level of Spo0A∼P thus functions as a developmental checkpoint in the response to starvation conditions.

In the next section, we review current knowledge on the network of interactions controlling the choice between vegetative growth and sporulation. In section 3, the qualitative simulation method described in [10] is briefly summarized. In sections 4 and 5, we show how the sporulation initiation network can be modeled in terms of PL models. The results obtained when simulating the bacterium in various genetic backgrounds are presented in section 6, followed by a discussion in the concluding section of the report.

2 Initiation of sporulation in *B. subtilis*

One of the most intriguing questions of modern biology concerns the decision-making processes involved in the adaptation of an organism to its environment. In order to survive, in the short term as well as on an evolutionary time scale, an organism constantly has to adapt to ever-changing conditions. The key to its adaptability is the capacity to monitor the environment and respond to changes in, for example, nutrient availability, cell density, temperature, and light by adjusting the synthesis and degradation of regulatory proteins controlling growth, metabolism, and development.

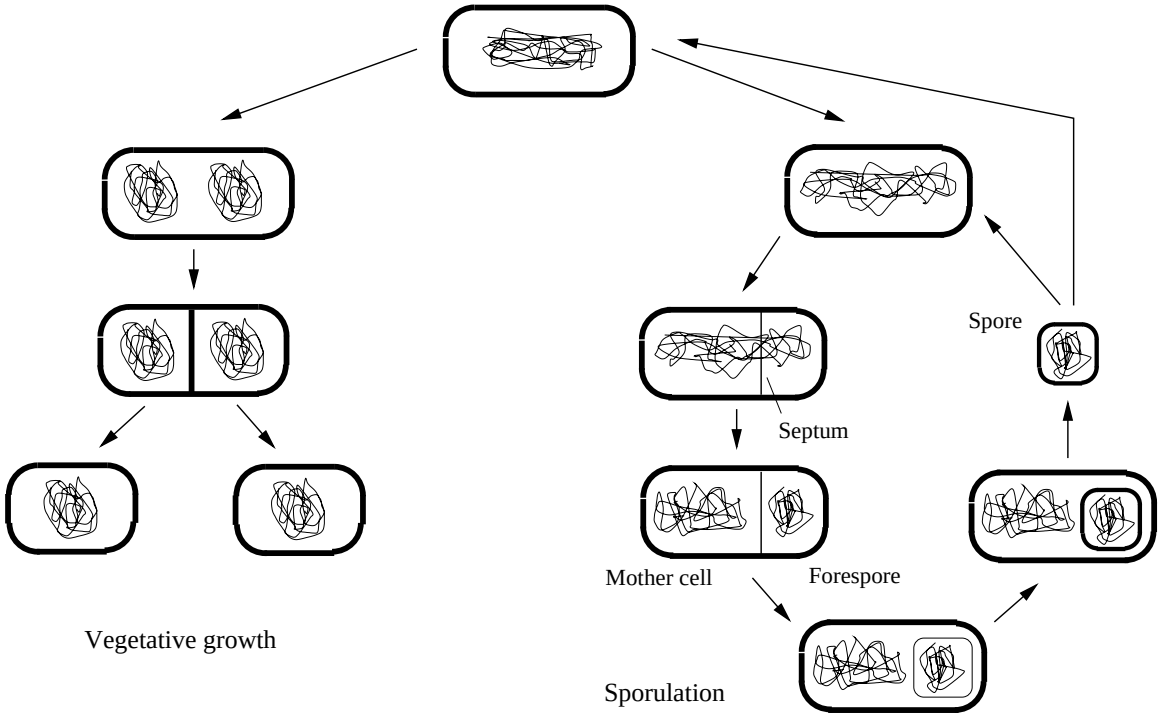

Figure 1: Life cycle of *B. subtilis*: decision between vegetative growth and sporulation (figure adapted from [48]).

Like any bacterium, *B. subtilis* is in constant competition with individuals of the same and different species for limited resources. As long as nutrients are available, *B. subtilis* cells growth and divide as fast as possible. However, when the environmental conditions deteriorate, the cells stop growing exponentially and enter stationary phase. During the transition to stationary phase, the cells initiate a range of responses destined to survive in the increasingly hostile environment [28, 32, 64, 72, 75]. The ultimate response of the cells is to *sporulate* [5, 28, 35, 76, 77], that is, to form spores that are remarkably resistant to chemicals, heat, dessication, radiation. Spores can remain dormant for many

years, but when the nutrient limitations disappear, the spores germinate and the bacterium resumes vegetative growth. In a bacterial culture submitted to starvation conditions, most of the cells will undergo sporulation (*spo*$^+$ phenotype), but a minority continues vegetative growth (*spo*$^-$ phenotype).

The morphological differences characterizing the *spo*$^+$ and *spo*$^-$ phenotypes can be easily identified (figure 1). During vegetative growth, the cell divides symmetrically and generates two identical cells. In sporulation, on the other hand, cell division is asymmetric and results in two different cell types: the smaller cell (the *forespore*) will form the spore, whereas the larger cell (the *mother cell*) helps to deposit a resistant coat around the spore and then disintegrates.

The decision to abandon vegetative growth and initiate sporulation involves a radical change in the genetic program, the pattern of gene expression, of the cell. The switch of genetic program is controlled by a complex genetic regulatory network involving more than 125 genes [17, 77]. Due to the ease of genetic manipulation of *B. subtilis*, it has been possible to identify and characterize a large number of the genes, proteins, and interactions making up this network. The decision-making processes involved in the choice between sporulation and vegetative growth have thus become a model for understanding the principles that underlie developmental decisions in higher organisms.

A crucial factor in the decision to commit the cell to sporulation is the phosphorylation of the transcription factor Spo0A in response to various environmental, cell-cycle, and metabolic signals [5, 28, 35, 76]. Above a certain threshold concentration, the phosphorylated protein activates a cascade of sigma factors directing the transcription of genes initiating the morphological changes occurring during sporulation [30, 43]. Spo0A∼P promotes the synthesis of σ^H, involved in septum formation and in the autoregulatory feedback loops controlling Spo0A∼P accumulation (see below). It also activates the genes coding for σ^E and σ^F, which are responsible for the alternative developmental fates of the mother cell and the forespore, respectively. Among other things, they activate the expression of yet other sigma factors, σ^K and σ^G, controlling late sporulation events. In this report, we will focus on the initial stage of sporulation, and consider that the cell is committed to sporulation once the concentration of σ^F has reached a certain threshold.

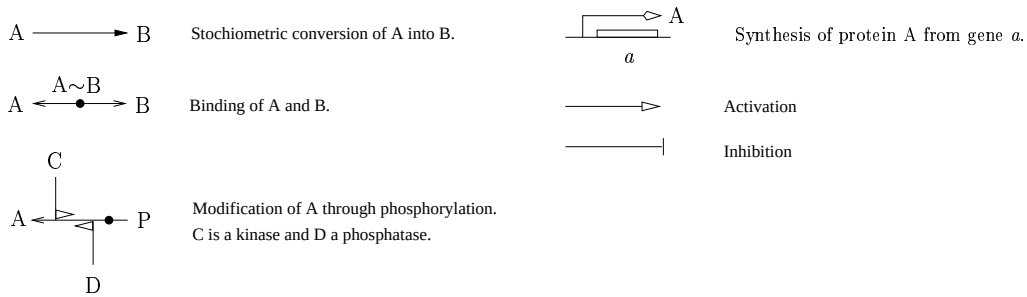

Figure 2: Elements of a graphical representation of genetic regulatory networks [42].

Figure 3 depicts key genes, proteins, and interactions involved in the initiation of sporulation, using the graphical conventions proposed by Kohn [42] (figure 2). The sporulation network is centered around a *phosphorelay*, responsible for the phosphorylation of Spo0A [4, 28, 35]. The phosphorelay transfers a phosphate from the kinase KinA, KinB, or KinC to the response regulator Spo0F, which in turn passes its phosphate to Spo0A, by way of the phosphotransferase Spo0B. The phosphatases Spo0E, RapA, and RapB, acting upon Spo0A∼P or Spo0F∼P, are able to reverse the flux of phosphate through the phosphorelay, thereby inactivating Spo0A. The activation of the kinases and phosphatases is determined by signals providing information about, among other things, nutrient availability, population density, progression of the cell cycle, and activity of metabolic pathways. The phosphorelay thus functions as an integrating device, deciding on the basis of a range of physiological and environmental parameters when it is appropriate for the cell to enter sporulation. Recent work has provided insights into the mechanisms connecting these parameters to the phosphorelay, although many of the molecular details remain unknown [5, 15, 28, 48, 76].

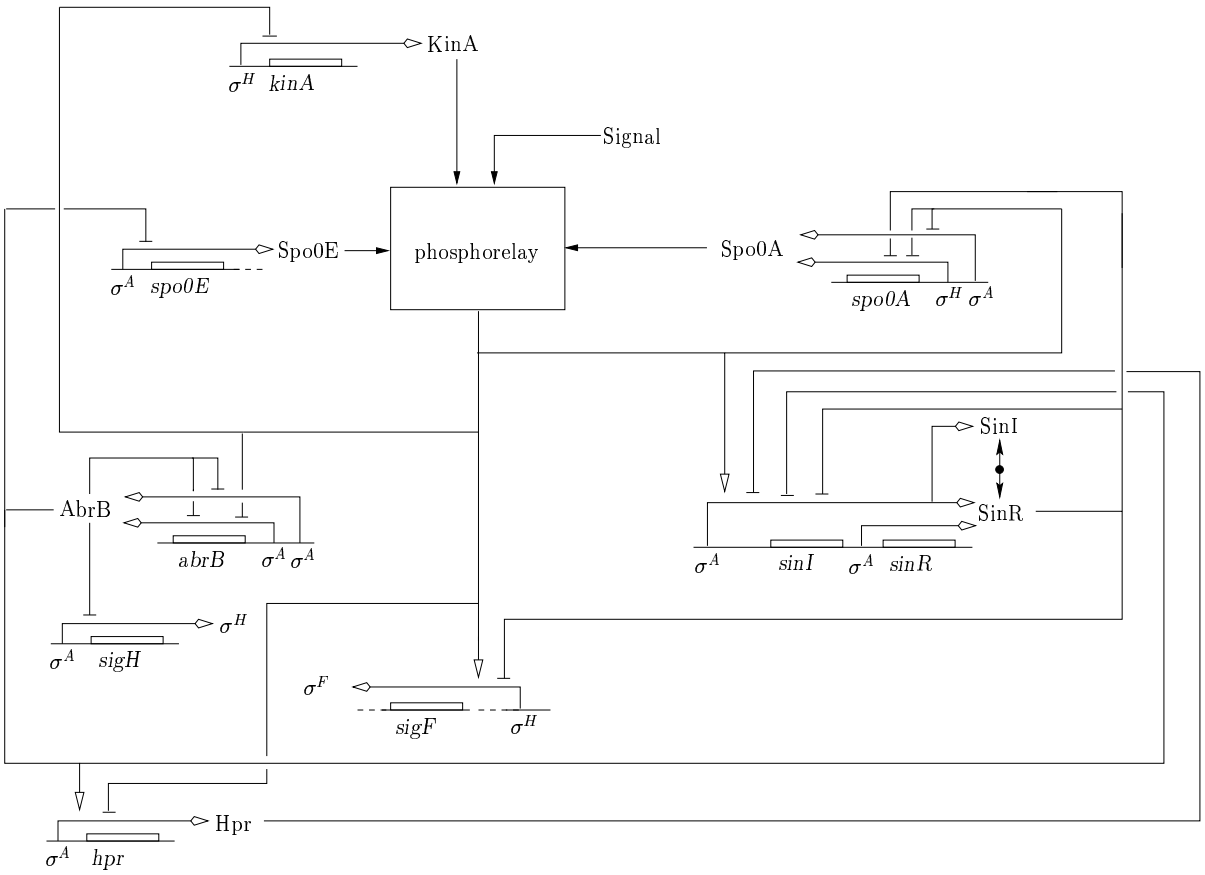

Figure 3: Network of key genes, proteins, and regulatory interaction involved in the initiation of sporulation in *B. subtilis*. The contents of the box denoting the phosphorelay are detailed in figure 4. In order to improve the legibility of the figure, the control of transcription by the sigma factors σ^A and σ^H has been represented implicitly, by annotating the promoter with the sigma factor in question.

The complexity of the phosphorelay, in comparison with the two-component systems usually responsible for signal transduction in bacteria, reflects the importance of the decision to commit the cell to sporulation [4]. The cell must balance the risk of unnecessarily initiating a process that confers a serious growth disadvantage against the risk of reacting too late to a disruptive change in environmental conditions. In this report, we simplify the phosphorelay by considering only one kinase (KinA) and one phosphatase (Spo0E), and by ignoring the intermediate steps in the transfer of phosphate to Spo0A (figure 4). This simplification does not affect the essential function of the phosphorelay: modulating the phosphate flux as a function of the competing action of kinases and phosphatases (here KinA and Spo0E) [57]. We also include one environmental signal, abbreviated to Signal, which acts on KinA and stimulates its autophosphorylation [89].

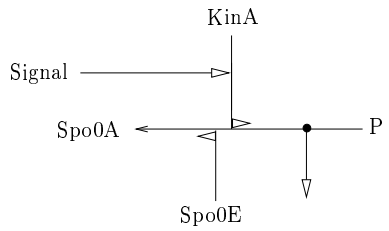

Figure 4: Simplified phosphorelay involved in *B. subtilis* sporulation. The intermediate steps in the transfer of phosphate to Spo0A have been compiled into a single step. Moreover, a single kinase (KinA), phosphatase (Spo0E), and environmental signal (Signal) are taken into account.

The components of the phosphorelay are themselves regulated on the transcriptional level by Spo0A∼P and a number of proteins directly or indirectly controlled by Spo0A∼P (figure 3). The transition-state regulator AbrB [78] plays a key role, in that it represses the expression of *spo0E*. In addition, it represses the gene *sigH*, which codes for the sigma factor σ^H directing the transcription of *kinA*, *spo0A*, and *sigF*. AbrB also controls the expression of other transition-state regulator genes [28, 64, 72, 79, 80], such as *sinR*, *sinI*, and *hpr*, which are involved in the regulation of the expression of *spo0A* from its σ^H-dependent promoter. More particularly, *sinR* codes for a repressor (SinR) of *spo0A* transcription and an anti-repressor (SinI). When SinR is complexed to SinI, it can no longer bind to DNA and repress transcription of *spo0A*. Hpr is a DNA-binding protein repressing the transcription of the *sinIR* operon [3]. In addition, the expression of *abrB* and most of the other genes mentioned above is positively or negatively controlled by Spo0A∼P [35].

How does the decision to enter sporulation or continue vegetative growth emerge from these interactions? Three feedback loops are particularly important for the accumulation of Spo0A∼P, and thereby the activation of the transcription of *sigF* and the commitment to sporulation [28, 36]. A first positive feedback loop arises from the downregulation of *abrB* following an increase in the concentration of Spo0A∼P. This leads to an increased expression of *sigH* and thereby *kinA*, which further stimulates phosphorylation of Spo0A. The downregulation of *abrB* and upregulation of *sigH* also give rise to a second positive feedback loop. A decrease in the concentration of *abrB* by Spo0A∼P leads to increased transcription of *hpr*, *sinI*, and *sinR*. Because *sinR* mRNA is poorly translated in comparison with *sinI* mRNA, most SinR will be inactivated through heterodimerization with SinI. As a consequence, following the upregulation of *sigH*, SinR repression of the σ^H-dependent promoter of *spo0A* is relieved. The increase in the concentration of Spo0A tends to augment the flux of phosphate through the phosphorelay. A third feedback loop involves an increase in *spo0E* expression caused by *abrB* downregulation through the phosphorelay. The feedback loop is negative, because increased concentrations of Spo0E opposes the accumulation of Spo0A∼P. Besides the three feedback loops mentioned above, there are other examples of (negative) feedback in the sporulation network, such as the repression of of *kinA* and *spo0A* transcription at high concentrations of Spo0A∼P.

The above description of the interactions in figure 3 has been much simplified (more details will be given in section 5), but it shows already that intuitive predictions of the global behavior of the system may be extraordinarily difficult to make. In order to understand how the choice between sporulation and vegetative growth emerges from the interplay of the competing feedback loops, we will build a mathematical model of the regulatory network and simulate the behavior of the system. We use the qualitative simulation method described in the accompanying report [10] for this purpose, because quantitative data on kinetic parameters and molecular concentrations are mostly absent.

3 Qualitative simulation of genetic regulatory networks

The qualitative simulation method in [10] is based on a class of piecewise-linear (PL) differential equation models that provide a coarse-grained description of genetic regulatory networks. The PL models have mathematical properties that allow qualitative predictions on the steady-state and transient behavior of the system to be made. Below, we give a brief summary of the method, focusing on the description of genetic regulatory networks by PL models (sections 3.1 and 3.2) and the predictions obtained through qualitative simulation (section 3.3).

3.1 Differential equation models

The dynamics of genetic regulatory networks can be modeled by a class of piecewise-linear (PL) differential equations originally proposed by Glass and Kauffman [25], and generalized by Mestl *et al.* [54]. The equations have the form

$$\dot{x}_i = f_i(\boldsymbol{x}, \boldsymbol{u}) - g_i(\boldsymbol{x}, \boldsymbol{u})\, x_i, \quad x_i \geq 0,\ 1 \leq i \leq n, \tag{1}$$

where $\boldsymbol{x} = (x_1, \ldots, x_n)'$ and $\boldsymbol{u} = (u_1, \ldots, u_m)'$ are vectors of cellular protein concentrations. The variables $\boldsymbol{x}$ represent the state of the regulatory system, whereas the variables $\boldsymbol{u}$ represent the input to the system. The *state equations* (1) define the rate of change of the concentration x_i as the difference of the rate of synthesis $f_i(\boldsymbol{x}, \boldsymbol{u})$ and the rate of degradation $g_i(\boldsymbol{x}, \boldsymbol{u})\, x_i$ of the protein. In what follows, we will assume that the input variables are constant, *i.e.*, $\dot{\boldsymbol{u}} = \boldsymbol{0}$.

The function $f_i : \mathbb{R}^n_{\geq 0} \times \mathbb{R}^m_{\geq 0} \to \mathbb{R}_{\geq 0}$ is defined as

$$f_i(\boldsymbol{x}, \boldsymbol{u}) = \sum_{l \in L} \kappa_{il}\, b_{il}(\boldsymbol{x}, \boldsymbol{u}), \tag{2}$$

where $\kappa_{il} > 0$ is a rate parameter, $b_{il} : \mathbb{R}^n_{\geq 0} \times \mathbb{R}^m_{\geq 0} \to \{0, 1\}$ a *regulation function*, and L a possibly empty set of indices of regulation functions. The regulation function is defined in terms of *step functions* $s^+, s^- : \mathbb{R} \times \mathbb{R} \to \{0, 1\}$, where

$$s^+(x_j, \theta_j) = \begin{cases} 1, & x_j > \theta_j, \\ 0, & x_j < \theta_j, \end{cases} \qquad \text{and} \qquad s^-(x_j, \theta_j) = 1 - s^+(x_j, \theta_j). \tag{3}$$

The parameter $\theta_j > 0$ represents a threshold concentration of x_j. A regulation function can be interpreted as the arithmetic equivalent of a Boolean function representing the logic of gene regulation [54, 74].

The function g_i is defined analogously to f_i, except that we demand that $g_i(\boldsymbol{x}, \boldsymbol{u})$ is strictly positive. In addition, in order to formally distinguish degradation rates from synthesis rates, we will denote the former by γ instead of κ. As can be easily verified, with the above definitions of f_i and g_i, differential equations of the form (1) are *piecewise-linear (PL)* [25, 54, 74].

The dynamical properties of the PL models can be analyzed in the n-dimensional phase space box $\Omega = \Omega_1 \times \ldots \times \Omega_n$, where every Ω_i, $1 \leq i \leq n$, is defined as

$$\Omega_i = \{x_i \in \mathbb{R}_{\geq 0} \mid 0 \leq x_i \leq max_i\}, \tag{4}$$

and max_i is a parameter denoting a maximum concentration for the protein.

Given that the protein encoded by gene i has p_i threshold concentrations, the $n-1$-dimensional threshold hyperplanes $x_i = \theta_i^{k_i}$, $1 \leq k_i \leq p_i$, partition Ω into hyperrectangular regions that are called *domains* [10, 54]. More precisely, a domain $D \subseteq \Omega$ is defined by $D = D_1 \times \ldots \times D_n$, where every D_i, $1 \leq i \leq n$, is given by one of the equations below:

$$\begin{aligned} D_i =& \{x_i \mid 0 \leq x_i < \theta_i^1\}, \\ D_i =& \{x_i \mid x_i = \theta_i^1\}, \\ D_i =& \{x_i \mid \theta_i^1 < x_i < \theta_i^2\}, \\ & \ldots \\ D_i =& \{x_i \mid \theta_i^{p_i} < x_i \leq max_i\}. \end{aligned} \tag{5}$$

If for a domain D, there are some i, j, $1 \leq i \leq n$, $1 \leq j \leq p_i$, such that $D_i = \{x_i \mid x_i = \theta_i^j\}$, then D is called a *switching* domain. Otherwise, D is called a *regulatory domain*.

When evaluating the step function expressions in (2) in a regulatory domain, f_i and g_i reduce to sums of rate constants. More precisely, in every regulatory domain $D \subseteq \Omega$, f_i reduces to some $\mu_i^D \in M_i \equiv \{f_i(\boldsymbol{x}) \mid \boldsymbol{0} \leq \boldsymbol{x} \leq \boldsymbol{max}\}$, and g_i to some $\nu_i^D \in N_i \equiv \{g_i(\boldsymbol{x}) \mid \boldsymbol{0} \leq \boldsymbol{x} \leq \boldsymbol{max}\}$. M_i and N_i collect the synthesis and degradation rates of the protein in different domains of Ω. It can be easily shown that all trajectories in D monotonically tend towards a stable steady state $\boldsymbol{x} = \boldsymbol{\mu}^D/\boldsymbol{\nu}^D$, the *target equilibrium*, lying at the intersection of the n hyperplanes $x_i = \mu_i^D/\nu_i^D$ [25, 54, 74]. The target equilibrium level μ_i^D/ν_i^D of the protein concentration x_i gives an indication of the strength of gene expression in D. Call $\Phi(D) = \{\boldsymbol{\mu}^D/\boldsymbol{\nu}^D\}$ the *target equilibrium set* of D. If $\Phi(D) \cap D \neq \{\}$, then all trajectories will remain in D. If not, they will leave D at some point.

In switching domains, f_i and g_i may not be defined, because some concentrations assume their threshold value. Moreover, the functions may be discontinuous. In order to cope with this problem, the system of differential equations (1) is extended into a system of differential inclusions, following an approach originally proposed by Filippov [19, 26]. Using this generalization, it can be shown that, in the case of a switching domain D, the trajectories either traverse D instantaneously or tend towards a target equilibrium set $\Phi(D)$ located in the same threshold hyperplane as D. Here, $\Phi(D)$ is the smallest closed convex set including the target equilibria of regulatory domains having D in their boundary. If $\Phi(D) \cap D \neq \{\}$, then the trajectories may remain in D. If not, they will leave D at some point.

3.2 Qualitative constraints on parameters

Most of the time, precise numerical values for the threshold and rate parameters in (1) are not available. As a consequence, it is not possible to numerically simulate the behavior of a genetic regulatory network. Rather than numerical values, we specify qualitative constraints on the parameter values. These constraints, having the form of algebraic inequalities, can usually be inferred from biological data. They are exploited by the simulation method to predict the qualitative dynamics of the regulatory system.

The first type of constraints, the *threshold inequalities*, are obtained by ordering the p_i threshold concentrations of the protein encoded by gene i, *i.e.*,

$$0 < \theta_i^1 < \ldots < \theta_i^{p_i} < max_i, \tag{6}$$

The threshold inequalities determine the partitioning of Ω into regulatory and switching domains.

The second type of constraints, the *equilibrium inequalities*, order the possible target equilibrium levels of x_i in different regulatory domains $D \subseteq \Omega$ with respect to the threshold concentrations. Biologically speaking, the equilibrium inequalities define the strength of gene expression in the domain in a qualitative way, on the scale of ordered threshold concentrations. More precisely, for every $\mu_i \in M_i$, $\nu_i \in N_i$, and $\mu_i, \nu_i \neq 0$, we specify one of the following pairs of inequalities:

$$\begin{aligned} &0 < \mu_i/\nu_i < \theta_i^1, \\ &\theta_i^1 < \mu_i/\nu_i < \theta_i^2, \\ &\dots \\ &\theta_i^{p_i} < \mu_i/\nu_i < max_i. \end{aligned} \tag{7}$$

The equilibrium inequalities constrain the relative position of D and its target equilibrium set $\Phi(D)$.

The models of genetic regulatory networks treated by the simulation method consist of state equations (1), supplemented by parameter inequalities (6) and (7). Every such *qualitative* PL model corresponds to a set of *quantitative* PL models consisting of state equations (1) and a particular combination of numerical parameter values consistent with the parameter inequalities.

3.3 Qualitative simulation

Let $\boldsymbol{x}$, defined on some time-interval $[0, \tau[$, be a solution of a quantitative PL model describing a genetic regulatory network. Furthermore, at some time-point t, $0 \leq t < \tau$, $\boldsymbol{x}(t) \in D$. A qualitative description of $\boldsymbol{x}$ at t consists of the domain D, supplemented by the relative position of D and $\Phi(D)$. We call this the *qualitative state* of the system. On $[0, \tau[$, the solution passes through a sequence of domains $D^0, \dots, D^m$ in Ω. Whenever $\boldsymbol{x}$ enters a new domain, the system makes a transition to a new qualitative state. The sequence of qualitative states corresponding to the sequence of domains is called the *qualitative behavior* of the system on the time-interval. Every solution of a quantitative PL model can be uniquely abstracted into a qualitative behavior.

Given a qualitative PL model and initial conditions in a domain D^0, the aim of *qualitative simulation* is to determine the possible qualitative behaviors of the system. More precisely, denoting by X the set of solutions $\boldsymbol{x}(t)$ of all quantitative PL models corresponding to the qualitative model, such that $\boldsymbol{x}(0) = \boldsymbol{x}_0 \in D^0$, the aim of qualitative simulation is to find the set of qualitative behaviors that abstract from some $\boldsymbol{x} \in X$.

In the accompanying report, we have described a simulation algorithm that generates a set of qualitative behaviors by recursively determining qualitative states and transitions from qualitative states, starting at the qualitative state associated with the initial domain D^0. This results in a *transition graph*, a directed graph of qualitative states and transitions between qualitative states. The transition graph contains *qualitative equilibrium states* or *qualitative cycles*. These may correspond to equilibrium points or limit cycles reached by solutions in X, and hence indicate functional modes of the regulatory system.

A sequence of qualitative states in the transition graph represents a predicted qualitative behavior of the system. It has been demonstrated that the transition graph generated by the simulation algorithm covers all qualitative behaviors abstracting from some $\boldsymbol{x} \in X$ [10]. That is, whatever the exact numerical values for the parameters may be, if these values are consistent with the threshold and equilibrium inequalities specified in the qualitative PL model, the qualitative shape of the solution is described by a sequence of states in the transition graph. On the other hand, the transition graph resulting from a simulation may contain more qualitative behaviors than necessary to cover the solutions in X [10].

The simulation method has been implemented in Java 1.3, in a program called *GNA (Genetic Network Analyzer)* [9].[1] GNA is accessible through a graphical user-interface, which displays the network of interactions among genes and proteins, as well as the transition graph resulting from the simulation. In addition, the user can analyze the qualitative equilibrium states and qualitative cycles, and focus on selected qualitative behaviors in order to study the temporal evolution of protein concentrations in more detail.

4 Modeling regulatory mechanisms in sporulation

In this section, we will discuss how the different types of interactions playing a role in the initiation of sporulation can be modeled in terms of step functions. More particularly, we will explain how the functions f_i in (1) can be specified when dealing with the regulation of gene expression by a transcriptional activator (section 4.1), a transcriptional repressor inactivated through dimerization with an anti-repressor (section 4.2), and a transcriptional repressor activated through a phosphorelay (sections 4.3). The resulting model components are combined in the next section, where for each of the proteins in the sporulation network a state equation will be defined.

4.1 Transcription regulator

Consider the transcription regulator AbrB that activates the expression of *hpr* by binding to a regulatory site in the promoter region of the gene [81]. This regulatory mechanism, schematically shown in figure 5(a), can be modeled by means of a sigmoidal function, the Hill rate law (appendix A.1). Figure 6(a) shows the activity of the gene, and hence the rate of synthesis of the protein, as a function of the cellular concentration x_{ab} of AbrB. Below a certain threshold concentration of the transcriptional regulator, *hpr* will be hardly expressed at all, whereas above this threshold its expression rapidly saturates.

Figure 5: Regulation of the expression of (a) *hpr* and (b) *abrB*.

The sigmoid curve in the figure can be conveniently approximated by a step function [39, 85]. This leads to the following expression for the rate of synthesis of Hpr:

$$f_{hr}(x_{ab}) = \kappa_{hr}\, s^{+}(x_{ab}, \theta^1_{ab}), \tag{8}$$

where κ_{hr} and θ^1_{ab} are constants denoting the synthesis rate of Hpr and the threshold concentration of AbrB, respectively. The function $f_{hr}(x_{ab})$ states that *hpr* is expressed at a rate κ_{hr}, if $x_{ab} > \theta^1_{ab}$, whereas the gene is not expressed, if $x_{ab} < \theta^1_{ab}$.

In addition to activating *hpr*, AbrB has been shown to inhibit its own synthesis, by binding to the promoter region of *abrB* [82]. As in the previous example, the activity plot of *abrB* is a sigmoidal curve (figure 6(b)). However, the synthesis of AbrB is now a decreasing function of the concentration of AbrB. Moreover, the curve is shifted to a higher concentration range. This reflects the observation that AbrB interacts more weakly with the promoter region of *abrB* than with that of *hpr*. The sigmoidal curve in figure 6(b) can be approximated by the step function expression

[1] GNA is available for non-profit academic research purposes at `http://www-helix.inrialpes.fr/gna`.

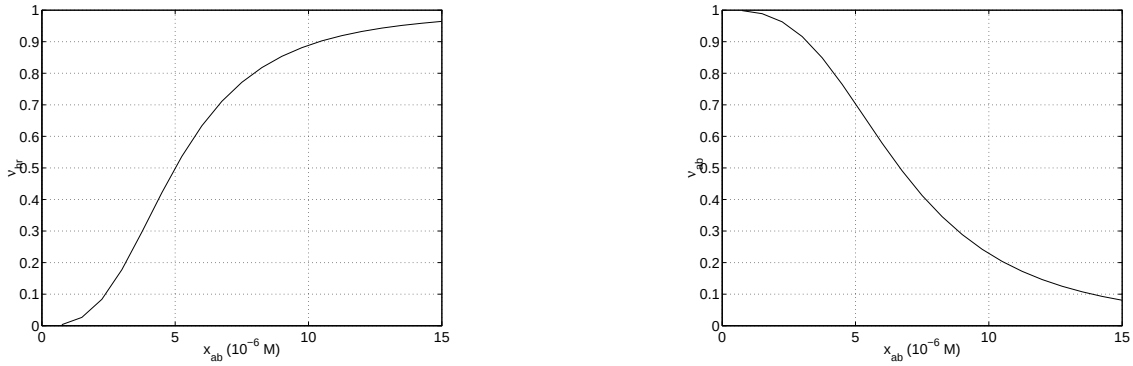

(a) (b)

Figure 6: (a) Activity of the gene *hpr* (ν_{hr}), normalized on the scale 0 to 1, as a function of the concentration of the transcriptional regulator AbrB (x_{ab}). (b) Idem for the activity of the gene *abrB* (ν_{ab}). The activity plots have been generated from the model and parameter values in appendix A.1. They correspond to the regulatory mechanisms in figure 5.

$$f_{ab}(x_{ab}) = \kappa_{ab}\, s^{-}(x_{ab}, \theta^2_{ab}), \tag{9}$$

where κ_{ab} denotes a synthesis rate, θ^2_{ab} a threshold concentration, and $\theta^2_{ab} > \theta^1_{ab}$.

The expression of *abrB* is also inhibited by Spo0A~P, while σ^A is required to inititate transcription of the gene. These interactions have been omitted for the purpose of this example. In section 5, we will extend (8) and (9) into complete descriptions of the regulatory logic of *hpr* and *abrB*.

4.2 Transcription regulator inactivated by anti-repressor

Figure 7 illustrates a more complex regulatory mechanism. The DNA-binding protein SinR inhibits the expression of the gene *spo0A* [52], as well as its own gene *sinR* [73, 70]. Binding of SinI to SinR causes the latter to lose its ability to repress the expression of *spo0A* and *sinR* [3]. That is, the regulatory protein SinR occurs in two forms: a free (active) form and a complexed (inactive) form.

(a) (b)

Figure 7: Regulatory mechanisms controlling the expression of (a) *spo0A* and (b) *sinR*.

Using the law of mass action and the Hill rate law, a detailed kinetic model for the above regulatory mechanism has been derived (appendix A.2). Because the association of SinR and SinI, and the dissociation of their complex, takes place on a time-scale largely inferior to the time-scale of the synthesis and degradation of the proteins, we can assume that the former processes are in quasi-equilibrium with respect to the latter [33, 68]. This gives rise to a simplified model which can be used to calculate, for arbitrary but realistic parameter values, the activity of *spo0A* as a function of the total SinR and SinI concentrations (x_{sr} and x_{si}). The resulting gene activity plot is shown in figure 8(a).

As a generalization of the previous example, the sigmoidal surface in the plot can be approximated by means of step functions. This leads to the following expression for the rate of synthesis of Spo0A:

$$f_{sa}(x_{sr}, x_{si}) = \kappa_{sa}\,(1 - s^{+}(x_{sr}, \theta^{2}_{sr})\, s^{-}(x_{si}, \theta^{1}_{si})), \tag{10}$$

with κ_{sa} a rate parameter and θ^{2}_{sr}, θ^{1}_{si} threshold concentrations. The function $f_{sa}(x_{sr}, x_{si})$ states that *spo0A* is expressed at a rate κ_{sa}, if $x_{sr} < \theta^{2}_{sr}$ or $x_{si} > \theta^{1}_{si}$. If this condition is not satisfied, the gene is not expressed.

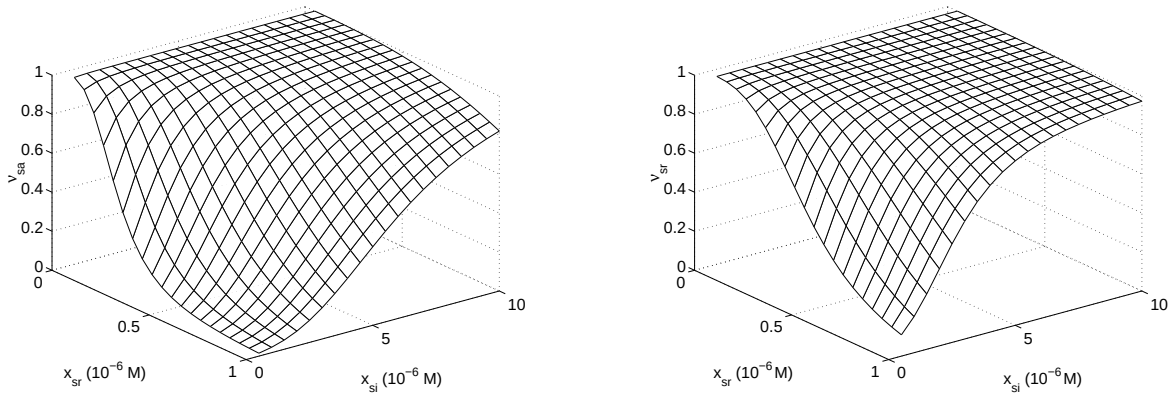

(a) (b)

Figure 8: (a) Activity of the gene *spo0A* (ν_{sa}), normalized on the scale 0 to 1, as a function of the concentrations of total SinR (x_{sr}) and total SinI (x_{si}). (b) Idem for the activity of the gene *sinR* (ν_{sr}). The activity plots have been produced using the kinetic model and parameter values in appendix A.2. They correspond to the regulatory mechanisms in figure 7.

Now consider the negative autoregulation of SinR shown in figure 7(b). SinR is assumed to bind more weakly to the promoter region of its own gene than to that of *spo0A*. Using the above-mentioned model to determine the gene activity plots, we obtain a sigmoidal surface shifted to a different region of the concentration space, as shown in figure 8(b). The corresponding step function expression approximation is

$$f_{sr}(x_{sr}, x_{si}) = \kappa_{sr}\,(1 - s^{+}(x_{sr}, \theta^{1}_{sr})\, s^{-}(x_{si}, \theta^{2}_{si})), \tag{11}$$

with $\theta^{2}_{sr} > \theta^{1}_{sr}$ and $\theta^{2}_{si} < \theta^{1}_{si}$.

When comparing figure 7 with figure 3, we see that the former gives an incomplete picture of the control of expression of *spo0A* and *sinR*. Both genes are regulated in a complex manner, involving several promoters and regulatory proteins. In section 5, we will complete the partial descriptions of the control of *spo0A* and *sinR* derived above.

4.3 Transcription regulator phosphorylated through phosphorelay

As discussed in section 2, the phosphorelay is the principal regulatory mechanism in the network controlling the initiation of sporulation. It controls the expression of various sporulation genes, such as the gene *sigF* included in the *spoIIA* operon [63, 86]. We consider the simplified version of the phosphorelay, shown in figure 4.

Although the phosphorelay is more complex than the regulatory mechanism of the previous section, a function summarizing the regulatory logic of *sigF* can be derived in much the same way. In appendix A.3, a detailed kinetic model for the regulation of *sigF* through the phosphorelay is derived from standard rate laws in enzyme kinetics. The model can be simplified by making the assumption, based on time-scale considerations, that the flux through the phosphorelay is in a state of quasi-equilibrium with respect to the synthesis and degradation of its component proteins. Given parameter

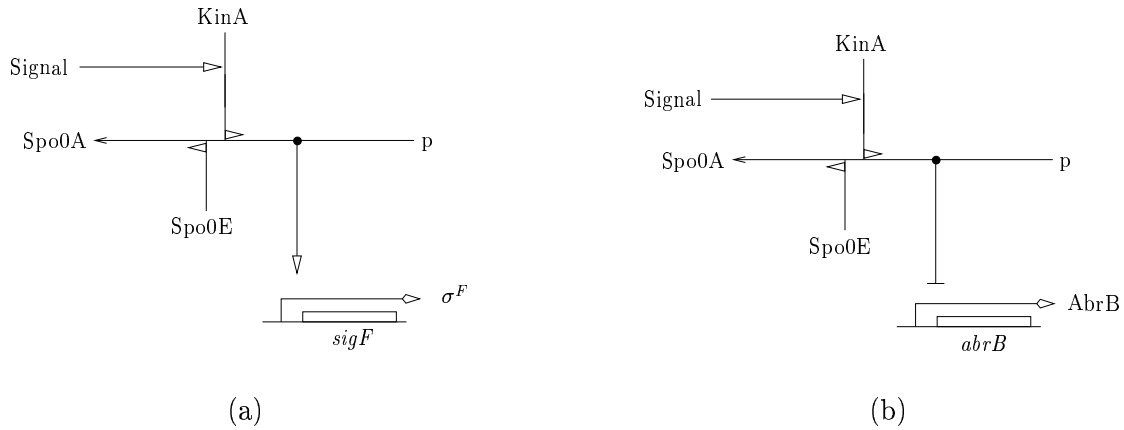

Figure 9: Control of the expression of (a) *sigF* and (b) *abrB* through the phoshorelay.

values consistent with the biochemical characterization of the interactions in [27], we calculate the activity of *sigF* as a function of the different concentrations of total Spo0A, total KinA, and total Spo0E (x_{sa}, x_{ka}, and x_{se}), in the absence and presence of Signal. The gene activity plots in figure 10(a)-(c) show that, if Signal is absent, then *sigF* is never expressed. On the other hand, if Signal is present, then we obtain the sigmoidal surfaces plotted in figure 10(d)-(f). The plots express the competition between the kinase and the phosphatase [57]: the activity of *sigF* increases with increasing concentrations of KinA and decreasing concentrations of Spo0E.

Let the input variable u_s denote the sporulation signal. We stipulate that the step function $s^+(u_s, \theta_s)$ evaluates to 1, if Signal is present, and to 0, if it is absent. Then the plots in figure 10 give rise to the following step function approximation for the rate of synthesis of σ^F:

$$f_f(x_{sa}, x_{ka}, x_{se}, u_s) = \kappa_f \, s^+(u_s, \theta_s) \, s^+(x_{sa}, \theta^3_{sa}) \, s^+(x_{ka}, \theta^3_{ka}) \, s^-(x_{se}, \theta^2_{se}). \tag{12}$$

κ_f is a rate parameter, while θ^3_{sa}, θ^3_{ka}, θ^2_{se} are threshold parameters for x_{sa}, x_{ka}, x_{se}, respectively. The function $f_f(x_{sa}, x_{ka}, x_{se}, u_s)$ formalizes the regulatory logic shown in the plots. In particular, if the sporulation signal is present ($s^+(u_s, \theta_s) = 1$), then gene *sigF* is expressed at a rate κ_f, if and only if $x_{sa} > \theta^3_{sa}$, $x_{ka} > \theta^3_{ka}$, and $x_{se} < \theta^2_{se}$. If the sporulation signal is absent ($s^+(u_s, \theta_s) = 0$), then *sigF* is not expressed.

Spo0A∼P has been shown to bind most strongly to the promoter region of *abrB*, thus making this gene a sensitive measure of Spo0A∼P accumulation in the cell [7, 87]. Repeating the above analysis for the transcriptional regulation of *abrB* by Spo0A∼P, as schematized in figure 9(b), results in gene activity plots analogous to those shown in figure 10 (results not shown). The sigmoidal curve is inversed, due to the fact that Spo0A∼P represses *abrB* expression. In addition, it is shifted to a different region of the concentration space, reflecting the stronger interaction of Spo0A∼P and the *abrB* promoter region. The regulatory logic of *abrB* is now approximated by

$$f_{ab}(x_{sa}, x_{ka}, x_{se}, u_s) = \kappa_{ab} \, (1 - s^+(u_s, \theta_s) \, s^+(x_{sa}, \theta^1_{sa}) \, s^+(x_{ka}, \theta^1_{ka}) \, s^-(x_{se}, \theta^4_{se})). \tag{13}$$

with $\theta^1_{sa} < \theta^3_{sa}$, $\theta^1_{ka} < \theta^3_{ka}$, and $\theta^4_{se} > \theta^2_{se}$.

The step function expressions (12)-(13) describe only part of the regulatory logic of the genes. In addition to being activated by Spo0A∼P, the expression of *sigF* is inhibited by SinR. Similarly, the expression of *abrB* is autoregulated through the action of AbrB. A complete description of the control of expression of these genes will be given in the next section, where the step function expression for Spo0A∼P regulation will be combined with those for SinR and AbrB regulation inferred above.

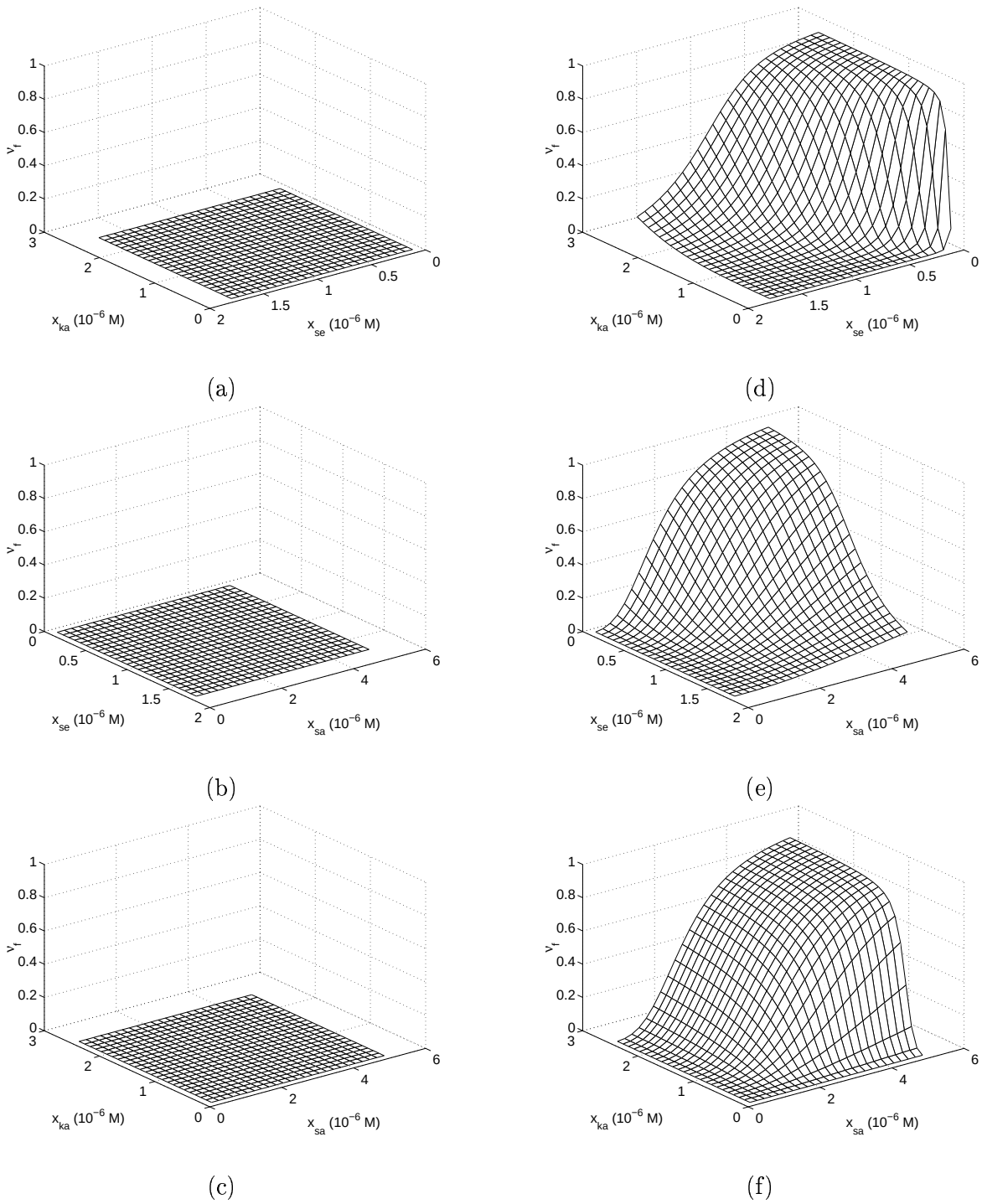

Figure 10: Activity of the gene *sigF*, normalized on the scale 0 to 1 (ν_f), as a function of the concentrations of total Spo0A (x_{sa}), total KinA (x_{ka}), and total Spo0E (x_{se}). In (a)-(c) Signal is present, whereas in (d)-(f) it is absent. The plots have been produced using the kinetic model and parameter values in appendix A.3. In each plot, two of the concentrations are varied while the third is held constant at the maximum or minimum value of the concentration range.

5 Modeling the sporulation network

In order to model the sporulation network of figure 3, we will define the state equation and parameter inequalities for the different classes of genes involved: the sigma factors σ^A, σ^H, and σ^F (section 5.1), the response regulator Spo0A (section 5.2), the kinase KinA (section 5.3), the phosphatase Spo0E (5.4), the transition state regulators AbrB, SinR, SinI, and Hpr (section 5.5), and the sporulation signal (section 5.6). The equations and inequalities making up the model are summarized in figure 11.

5.1 Sigma factors σ^A, σ^H, and σ^F

As reviewed in section 2, sporulation in *B. subtilis* requires the sequential activation of different sigma subunits of RNA polymerase [30, 43]. σ^A is the principal sigma factor present in vegetatively growing cells, but it has an ongoing role during sporulation [30]. For the purpose of this model, its concentration u_a will be considered constant, that is,

$$\dot{u}_a = 0. \tag{14}$$

σ^A is assigned a single threshold concentration θ_a, which leads to the straightforward threshold inequalities

$$0 < \theta_a < max_a. \tag{15}$$

If $x_a > \theta_a$, then σ^A is available at concentrations at which it can direct RNA polymerase to transcribe genes with a σ^A-dependent promoter. No equilibrium inequalities need to be specified for σ^A ($M_a = \{0\}$ and $N_a = \{0\}$).

The sigma factor σ^H, present at low concentrations in the growing cell, is essential for the initiation of sporulation [30, 43]. It is the product of the gene *sigH* (also known as *spo0H*), which is transcribed from a σ^A-dependent promoter [6, 14, 90]. Control of expression of *sigH* is regulated by AbrB, which represses transcription of the gene [21, 91]. We use the rate constants κ_h^0 and κ_h^1 to denote constitutive and AbrB-controlled synthesis of σ^H.[2] Degradation of σ^H is assumed to occur spontaneously, with a rate constant γ_h. This leads to the following state equation for σ^H:

$$\dot{x}_h = \kappa_h^0\, s^+(x_a, \theta_a) + \kappa_h^1\, s^+(x_a, \theta_a)\, s^-(x_{ab}, \theta_{ab}^1) - \gamma_h\, x_h. \tag{16}$$

The step function expressions for σ^A-dependent transcription and AbrB-effected repression, *i.e.*, $s^+(x_a, \theta_a)$ and $s^-(x_{ab}, \theta_{ab}^1)$, respectively, are multiplied, reflecting that the two mechanisms operate independently.

As in the case of σ^A, we define a single threshold concentration for σ^H. Above this concentration, denoted by θ_h, the σ^H-dependent promoters of the sporulation genes can be transcribed by the Eσ^H holoenzyme. This leads to the threshold inequalities

$$0 < \theta_h < max_h. \tag{17}$$

By means of (16), we derive the possible synthesis and degradation rates of σ^H, $M_h = \{0, \kappa_h^0, \kappa_h^0 + \kappa_h^1\}$ and $N_h = \{\gamma_h\}$. The target equilibrium values κ_h^0/γ_h and $(\kappa_h^0 + \kappa_h^1)/\gamma_h$ need to be ordered with respect to θ_h. The increased expression of *sigH* at the end of exponential growth, due to the relief of AbrB repression, is necessary for the initiation of sporulation [5, 28, 35]. This implies the constraints $\kappa_h^0/\gamma_h < \theta_h$ and $(\kappa_h^0 + \kappa_h^1)/\gamma_h > \theta_h$, and hence the equilibrium inequalities:

[2] Several reports indicate that the cellular concentration of σ^H, x_h, is also regulated on the post-transcriptional level (*e.g.*, [16, 31, 91]). Because the exact mechanisms involved have not been elucidated thus far [12, 16], we will omit this level of regulation.

$$0 < \frac{\kappa_h^0}{\gamma_h} < \theta_h, \quad \theta_h < \frac{\kappa_h^0 + \kappa_h^1}{\gamma_h} < max_h. \tag{18}$$

σ^F is a sigma factor controlling the development of the forespore [30, 43]. The operon *spoIIA* includes the gene *sigF* (*spoIIAC*) coding for σ^F [20]. Transcription of *spoIIA* is σ^H-dependent [93, 94] and positively controlled by Spo0A~P as well as negatively controlled by SinR [51, 63, 86, 94]. The synthesis rate of σ^F is denoted by κ_f, while σ^F is degraded with rate constant γ_f. Denoting the cellular concentration of σ^F by x_f, the state equation for σ^F is obtained by combining the step function expressions for Spo0A~P and SinR regulation derived in section 4:

$$\begin{aligned}\dot{x}_f = \kappa_f\, s^+(x_h, \theta_h)\,(1 - s^+(x_{sr}, \theta_{sr}^1)\, s^-(x_{si}, \theta_{si}^2))\cdot \\ s^+(u_s, \theta_s)\, s^+(x_{sa}, \theta_{sa}^3)\, s^+(x_{ka}, \theta_{ka}^3)\, s^-(x_{se}, \theta_{se}^2) - \gamma_f\, x_f.\end{aligned} \tag{19}$$

We define a single threshold θ_f for σ^F. At concentrations above this threshold, the sigma factor directs transcription of genes implicated in forespore development. The accumulation of σ^F above its threshold level will be taken to indicate the initiation of sporulation. The threshold inequalities for σ^F are

$$0 < \theta_f < max_f. \tag{20}$$

The possible synthesis and degradation rates of σ^F are $M_f = \{0, \kappa_f\}$ and $N_f = \{\gamma_f\}$. Because expression of *sigF* must allow the concentration of σ^F to cross the threshold θ_f, we obtain the equilibrium inequalities

$$\theta_f < \frac{\kappa_f}{\gamma_f} < max_f. \tag{21}$$

5.2 Response regulator Spo0A

Expression of the gene *spo0A* coding for Spo0A can be initiated from a σ^A-dependent (vegetative) promoter P_V and a σ^H-dependent (sporulation) promoter P_S [18, 44, 65, 71, 96]. We will use the rate constants κ_{sa}^1 and κ_{sa}^2 to denote the synthesis of Spo0A from P_V and P_S, respectively. Control of expression from P_V involves transcription by the $E\sigma^A$ holoenzyme [96] and repression by Spo0A~P [83]. Expression from P_S is controlled by three mechanisms: transcription by the $E\sigma^H$ holoenzyme [18, 65, 71, 96], repression by Spo0A~P [83], and repression by SinR [52].[3] Degradation of Spo0A turnover is not known to be regulated, so that we will assume spontaneous degradation with a rate constant γ_{sa}. Denoting by x_a the total concentration of Spo0A, we arrive at the following state equation:

$$\begin{aligned}\dot{x}_{sa} = \kappa_{sa}^1\, s^+(x_a, \theta_a)\,(1 - s^+(u_s, \theta_s)\, s^+(x_{sa}, \theta_{sa}^3)\, s^+(x_{ka}, \theta_{ka}^3)\, s^-(x_{se}, \theta_{se}^2)) + \\ \kappa_{sa}^2\, s^+(x_h, \theta_h)\,(1 - s^+(u_s, \theta_s)\, s^+(x_{sa}, \theta_{sa}^4)\, s^+(x_{ka}, \theta_{ka}^4)\, s^-(x_{se}, \theta_{se}^1))\cdot \\ (1 - s^+(x_{sr}, \theta_{sr}^1)\, s^-(x_{si}, \theta_{si}^2)) - \gamma_{sa}\, x_{sa}.\end{aligned} \tag{22}$$

Notice that the step function expressions for the different regulatory mechanisms are multiplied, in order to represent their combined effect in transcription control.

Spo0A~P has been shown to bind most strongly to the promoter region of the gene encoding the transition state regulator AbrB, while at a higher concentration level it starts to activate expression

[3] Although earlier experiments suggested that Spo0A~P also activates transcription from the P_S promoter, recent *in vivo* transcription analyses have not substantiated this conclusion [21].

of the gene coding for the sigma factor σ^F [7, 28, 86]. The latter event requires the positive feedback loop amplifying the flux of phosphate through the phosphorelay to have become active, and therefore downregulation of *hpr* and upregulation of *sinI* to have occurred at lower concentrations of Spo0A∼P [28, 35]. Once Spo0A∼P has reached concentration levels sufficient to activate *sigF*, it inhibit its further accumulation, by shutting off expression of the phosphorelay genes *spo0A* and *kinA* [28, 35]. Downregulation of the other promoter of *spo0A* occurs at a lower concentration of Spo0A∼P, at about the time that SinR repression of P_S is released and transcription from this promoter starts (promoter switching) [65, 96].

The above considerations lead us to distinguish four different strengths of Spo0A∼P binding, and hence (following the reasoning in section 4.3) to four different threshold concentrations for the phosphorelay proteins. In the case of Spo0A, we have the thresholds θ^1_{sa}, θ^2_{sa}, θ^3_{sa}, and θ^4_{sa}, which are ordered by the threshold inequalities

$$0 < \theta^1_{sa} < \theta^2_{sa} < \theta^3_{sa} < \theta^4_{sa} < max_{sa}. \tag{23}$$

The threshold θ^1_{sa} corresponds to *abrB* repression of Spo0A∼P, while θ^2_{sa} accounts for the regulation of the other transition state regulator genes. The Spo0A concentration must reach θ^3_{sa} to activate *sigF* expression and repress its own synthesis from the P_V promoter. Above θ^4_{sa}, it inhibits further expression of the phosphorelay genes, as can be verified in (22).

The possible synthesis and degradation rates of Spo0A are given by $M_{sa} = \{0, \kappa^1_{sa}, \kappa^2_{sa}, \kappa^1_{sa} + \kappa^2_{sa}\}$ and $N_{sa} = \{\gamma_{sa}\}$. We have to order the target equilibrium values $\kappa^1_{sa}/\gamma_{sa}$, $\kappa^2_{sa}/\gamma_{sa}$, and $(\kappa^1_{sa} + \kappa^2_{sa})/\gamma_{sa}$ with respect to the threshold values. Expression of Spo0A from the promoter P_V alone permits downregulation of *abrB* under the appropriate conditions, but is not sufficient to initiate sporulation [35, 87]. As can be verified in (31) and (19), this implies $\kappa^1_{sa}/\gamma_{sa} > \theta^1_{sa}$ and $\kappa^1_{sa}/\gamma_{sa} < \theta^3_{sa}$, respectively. It has been shown that expression from the promoter P_S is necessary to initiate sporulation [71]. Making the additional, reasonable assumption that the Spo0A∼P concentration may actually reach a level at which the negative feedback loop becomes active, (22) implies $\kappa^2_{sa}/\gamma_{sa} > \theta^4_{sa}$. In summary, we have the following equilibrium inequalities for Spo0A:

$$\theta^2_{sa} < \frac{\kappa^1_{sa}}{\gamma_{sa}} < \theta^3_{sa}, \quad \theta^4_{sa} < \frac{\kappa^2_{sa}}{\gamma_{sa}} < max_{sa}, \quad \theta^4_{sa} < \frac{\kappa^1_{sa} + \kappa^2_{sa}}{\gamma_{sa}} < max_{sa}. \tag{24}$$

Notice that $\kappa^2_{sa}/\gamma_{sa} > \theta^4_{sa}$ implies $(\kappa^1_{sa} + \kappa^2_{sa})/\gamma_{sa} > \theta^4_{sa}$.

5.3 Kinase KinA

Of the kinases mentioned in section 2, only the kinase considered to be most important, KinA, has been retained in the simplified phosphorelay. The gene *kinA* (*spoIIJ*) is transcribed from a σ^H-dependent promoter [2, 58, 65], repressed by Spo0A∼P [21, 35]. The degradation of the kinase is not known to be regulated. We introduce the variable x_{ka} to represent the concentration of total KinA. We denote the synthesis rate of KinA from its σ^H-dependent promoter by κ^1_{ka}. In addition, we introduce a synthesis rate κ^0_{ka} to account for the contribution of the kinases that have been omitted from the model, in particular KinB and KinC [37, 41, 46, 47, 87]. With a degradation rate equal to $\gamma_{ka}\, x_{ka}$, we obtain the state equation

$$\dot{x}_{ka} = \kappa^0_{ka}\, s^+(x_a, \theta_a) + \kappa^1_{ka}\, s^+(x_h, \theta_h)\, (1 - s^+(u_s, \theta_s)\, s^+(x_{sa}, \theta^4_{sa})\, s^+(x_{ka}, \theta^4_{ka})\, s^-(x_{se}, \theta^1_{se})) - \gamma_{ka}\, x_{ka}. \tag{25}$$

As explained in section 5.2, Spo0A∼P is assumed to interact at four different strengths with the promoter regions of its target genes, corresponding to four different concentration thresholds of the phosphorelay proteins. In the case of KinA, we have the thresholds θ^1_{ka}, θ^2_{ka}, θ^3_{ka}, and θ^4_{ka}, ordered by

$$0 < \theta^1_{ka} < \theta^2_{ka} < \theta^3_{ka} < \theta^4_{ka} < max_{ka}. \tag{26}$$

The possible synthesis and degradation rates of KinA are given by $M_{ka} = \{\kappa^0_{ka}, \kappa^1_{ka}, \kappa^0_{ka} + \kappa^1_{ka}\}$ and $N_{ka} = \{\gamma_{ka}\}$. Expression of *kinC* alone yields a Spo0A∼P level that is not sufficient to initiate sporulation, but that permits *abrB* downregulation [37, 47, 87]. From (19) and (31) we conclude that this implies $\kappa^0_{ka}/\gamma_{ka} < \theta^3_{ka}$ and $\kappa^0_{ka}/\gamma_{ka} > \theta^1_{ka}$. The expression of *kinA* alone allows the bacterium to sporulate under appropriate conditions [47, 87]. For *sigF* expression to occur, we must have $(\kappa^0_{ka} + \kappa^1_{ka})/\gamma_{ka} > \theta^3_{ka}$, while autoregulation of phosphorelay activity at higher concentrations of Spo0A∼P requires $(\kappa^0_{ka} + \kappa^1_{ka})/\gamma_{ka} > \theta^4_{ka}$. This gives rise to the following equilibrium inequalities:

$$\theta^2_{ka} < \frac{\kappa^0_{ka}}{\gamma_{ka}} < \theta^3_{ka}, \quad \theta^4_{ka} < \frac{\kappa^1_{ka}}{\gamma_{ka}} < max_{ka}, \quad \theta^4_{ka} < \frac{\kappa^0_{ka} + \kappa^1_{ka}}{\gamma_{ka}} < max_{ka}. \tag{27}$$

where we have made use of the implicit constraint $\kappa^0_{ka} + \kappa^1_{ka} > \kappa^1_{ka}$.

5.4 Phosphatase Spo0E

Historically, Spo0E is the first phosphatase that has been characterized. It is encoded by *spo0E*, a gene transcribed from a σ^A-dependent promoter [59] repressed by AbrB [61, 81]. Denoting by κ^0_{se}, κ^1_{se}, and γ_{se} the synthesis and degradation rate constants, we obtain the state equation

$$\dot{x}_{se} = \kappa^0_{se}\, s^+(x_a, \theta_a) + \kappa^1_{se}\, s^+(x_a, \theta_a)\, s^-(x_{ab}, \theta_{ab}) - \gamma_{se}\, x_{se}. \tag{28}$$

Like the other phosphorelay proteins, Spo0E has four threshold concentrations: θ^1_{se}, θ^2_{se}, θ^3_{se}, and θ^4_{se}. These are ordered by the threshold inequalities

$$0 < \theta^1_{se} < \theta^2_{se} < \theta^3_{se} < \theta^4_{se} < max_{se}. \tag{29}$$

The possible synthesis and degradation rates of Spo0E are given by $M_{se} = \{0, \kappa^0_{se}, \kappa^0_{se} + \kappa^1_{se}\}$ and $N_{se} = \{\gamma_{se}\}$, respectively. We will set $(\kappa^0_{se} + \kappa^1_{se})/\gamma_{se} > \theta^3_{se}$. If this were not the case, Spo0E would not be able to reach a concentration at which it can exert any influence on the sporulation decision [61]. In fact, as can be verified in (19), the state equation for σ^F, it must hold that $x_{se} > \theta^3_{se}$ for Spo0E to inhibit the initiation of sporulation. In addition, *spo0E* is expressed at a background level during vegetative growth [59]. This motivates the following equilibrium inequalities:

$$\theta^1_{se} < \frac{\kappa^0_{se}}{\gamma_{se}} < \theta^2_{se}, \quad \theta^3_{se} < \frac{\kappa^0_{se} + \kappa^1_{se}}{\gamma_{se}} < \theta^4_{se}. \tag{30}$$

5.5 Transition state regulators AbrB, SinR, SinI, and Hpr

The transition state regulators implicated in the decision to sporulate that have been best characterized are AbrB, SinR, SinI, and Hpr [28, 64, 72, 79, 80]. The gene *abrB* is transcribed from two vegetative-growth promoters, P1 and P2 [62, 78]. While the P2 promoter is repressed by both Spo0A∼P and AbrB itself, the P1 promoter is regulated by AbrB only [62, 81, 82]. We denote by κ^1_{ab} and κ^2_{ab} the synthesis constants for the P1 and P2 promoters, respectively, and by γ_{ab} the degradation constant. This gives the following state equation:

$$\begin{aligned}\dot{x}_{ab} = \kappa^1_{ab}\, s^+(x_a, \theta_a)\, s^-(x_{ab}, \theta^2_{ab}) + \kappa^2_{ab}\, s^+(x_a, \theta_a)\, s^-(x_{ab}, \theta^2_{ab}) \cdot \\ (1 - s^+(u_s, \theta_s)\, s^+(x_{sa}, \theta^1_{sa})\, s^+(x_{ka}, \theta^1_{ka})\, s^-(x_{se}, \theta^4_{se})) - \gamma_{ab}\, x_{ab}.\end{aligned} \tag{31}$$

AbrB has two threshold concentrations, θ^1_{ab} and θ^2_{ab}, which are ordered by the threshold inequalities

$\dot{u}_a = 0$ $0 < \theta_a < max_a$
$\dot{x}_h = \kappa_h^0\, s^+(x_a,\theta_a) + \kappa_h^1\, s^+(x_a,\theta_a)\, s^-(x_{ab},\theta_{ab}^1) - \gamma_h\, x_h$ $0 < \theta_h < max_h$ $0 < \kappa_h^0/\gamma_h < \theta_h, \quad \theta_h < (\kappa_h^0 + \kappa_h^1)/\gamma_h < max_h$
$\dot{x}_f = \kappa_f\, s^+(x_h,\theta_h)\,(1 - s^+(x_{sr},\theta_{sr}^1)\, s^-(x_{si},\theta_{si}^2))\cdot$ $\quad s^+(u_s,\theta_s)\, s^+(x_{sa},\theta_{sa}^3)\, s^+(x_{ka},\theta_{ka}^3)\, s^-(x_{se},\theta_{se}^2) - \gamma_f\, x_f$ $0 < \theta_f < max_f$ $\theta_f < \kappa_f/\gamma_f < max_f$
$\dot{x}_{sa} = \kappa_{sa}^1\, s^+(x_a,\theta_a)\,(1 - s^+(u_s,\theta_s)\, s^+(x_{sa},\theta_{sa}^3)\, s^+(x_{ka},\theta_{ka}^3)\, s^-(x_{se},\theta_{se}^2))+$ $\quad \kappa_{sa}^2\, s^+(x_h,\theta_h)\,(1 - s^+(u_s,\theta_s)\, s^+(x_{sa},\theta_{sa}^4)\, s^+(x_{ka},\theta_{ka}^4)\, s^-(x_{se},\theta_{se}^1))\cdot$ $\quad (1 - s^+(x_{sr},\theta_{sr}^1)\, s^-(x_{si},\theta_{si}^2)) - \gamma_{sa}\, x_{sa}$ $0 < \theta_{sa}^1 < \theta_{sa}^2 < \theta_{sa}^3 < \theta_{sa}^4 < max_{sa}$ $\theta_{sa}^2 < \kappa_{sa}^1/\gamma_{sa} < \theta_{sa}^3, \quad \theta_{sa}^4 < \kappa_{sa}^2/\gamma_{sa} < max_{sa}, \quad \theta_{sa}^4 < (\kappa_{sa}^1 + \kappa_{sa}^2)/\gamma_{sa} < max_{sa}$
$\dot{x}_{ka} = \kappa_{ka}^0\, s^+(x_a,\theta_a) + \kappa_{ka}^1\, s^+(x_h,\theta_h)\,(1 - s^+(u_s,\theta_s)\, s^+(x_{sa},\theta_{sa}^4)\, s^+(x_{ka},\theta_{ka}^4)\, s^-(x_{se},\theta_{se}^1)) - \gamma_{ka}\, x_{ka}$ $0 < \theta_{ka}^1 < \theta_{ka}^2 < \theta_{ka}^3 < \theta_{ka}^4 < max_{ka}$ $\theta_{ka}^2 < \kappa_{ka}^0/\gamma_{ka} < \theta_{ka}^3, \quad \theta_{ka}^4 < \kappa_{ka}^1/\gamma_{ka} < max_{ka}, \quad \theta_{ka}^4 < (\kappa_{ka}^0 + \kappa_{ka}^1)/\gamma_{ka} < max_{ka}$
$\dot{x}_{se} = \kappa_{se}^0\, s^+(x_a,\theta_a) + \kappa_{se}^1\, s^+(x_a,\theta_a)\, s^-(x_{ab},\theta_{ab}) - \gamma_{se}\, x_{se}$ $0 < \theta_{se}^1 < \theta_{se}^2 < \theta_{se}^3 < \theta_{se}^4 < max_{se}$ $\theta_{se}^1 < \kappa_{se}^0/\gamma_{se} < \theta_{se}^2, \quad \theta_{se}^3 < (\kappa_{se}^0 + \kappa_{se}^1)/\gamma_{se} < \theta_{se}^4$
$\dot{x}_{ab} = \kappa_{ab}^1\, s^+(x_a,\theta_a)\, s^-(x_{ab},\theta_{ab}^2) + \kappa_{ab}^2\, s^+(x_a,\theta_a)\, s^-(x_{ab},\theta_{ab}^2)\cdot$ $\quad (1 - s^+(u_s,\theta_s)\, s^+(x_{sa},\theta_{sa}^1)\, s^+(x_{ka},\theta_{ka}^1)\, s^-(x_{se},\theta_{se}^4)) - \gamma_{ab}\, x_{ab}$ $0 < \theta_{ab}^1 < \theta_{ab}^2 < max_{ab}$ $0 < \kappa_{ab}^1/\gamma_{ab} < \theta_{ab}^1, \quad \theta_{ab}^2 < (\kappa_{ab}^1 + \kappa_{ab}^2)/\gamma_{ab} < max_{ab}$
$\dot{x}_{sr} = \kappa_{sr}^0\, s^+(x_a,\theta_a) + \kappa_{sr}^1\, s^+(x_a,\theta_a)\, s^-(x_{ab},\theta_{ab}^1)\, s^-(x_{hr},\theta_{hr})\,(1 - s^+(x_{sr},\theta_{sr}^2)\, s^-(x_{si},\theta_{si}^1))\cdot$ $\quad (1 - s^+(u_s,\theta_s)\, s^+(x_{sa},\theta_{sa}^2)\, s^+(x_{ka},\theta_{ka}^2)\, s^-(x_{se},\theta_{se}^3)) - \gamma_{sr}\, x_{sr}$ $0 < \theta_{sr}^1 < \theta_{sr}^2 < max_{sr}$ $\theta_{sr}^2 < \kappa_{sr}^0/\gamma_{sr} < max_{sr}, \quad \theta_{sr}^2 < (\kappa_{sr}^0 + \kappa_{sr}^1)/\gamma_{sr} < max_{sr}$

Figure 11: State equations and parameter inequalities for the sporulation network of figure 3. The model has nine state variables and one exogenous variable corresponding to the concentrations of key proteins. An additional exogenous variable denotes the presence of a sporulation signal: x_{ka} (KinA), x_h (σ^H), x_{se} (Spo0E), x_{ab} (AbrB), x_{sa} (Spo0A), x_{si} (SinI), x_{sr} (SinR), x_{hr} (Hpr), x_f (σ^F), x_a (σ^A), x_s (Signal).

$\dot{x}_{si} = \kappa^0_{si}\, s^+(x_a,\theta_a) + \kappa^1_{si}\, s^+(x_a,\theta_a)\, s^-(x_{ab},\theta^1_{ab})\, s^-(x_{hr},\theta_{hr})\,(1 - s^+(x_{sr},\theta^2_{sr})\, s^-(x_{si},\theta^1_{si}))\cdot$ $(1 - s^+(u_s,\theta_s)\, s^+(x_{sa},\theta^2_{sa})\, s^+(x_{ka},\theta^2_{ka})\, s^-(x_{se},\theta^3_{se})) - \gamma_{si}\, x_{si}$ $0 < \theta^1_{si} < \theta^2_{si} < max_{si}$ $\theta^1_{si} < \kappa^0_{si}/\gamma_{si} < \theta^2_{si}, \quad \theta^2_{si} < (\kappa^0_{si} + \kappa^1_{si})/\gamma_{si} < max_{si}$
$\dot{x}_{hr} = \kappa_{hr}\, s^+(x_a,\theta_a)\, s^+(x_{ab},\theta^1_{ab})\, s^+(u_s,\theta_s)\, s^+(x_{sa},\theta^2_{sa})\, s^+(x_{ka},\theta^2_{ka})\, s^-(x_{se},\theta^3_{se}) - \gamma_{hr}\, x_{hr}$ $0 < \theta_{hr} < max_{hr}$ $\theta_{hr} < \kappa_{hr}/\gamma_{hr} < max_{hr}$
$\dot{u}_s = 0$ $0 < \theta_s < max_s$

Figure 11: Continued.

$$0 < \theta^1_{ab} < \theta^2_{ab} < max_{ab}. \tag{32}$$

The first threshold corresponds to concentrations above which AbrB represses *kinA*, *spo0E*, *sinR*, *sinI*, and *sigH*, while the second threshold corresponds to the concentration above which autorepression of *abrB* takes place [82].

The possible synthesis and degradation rates of AbrB are $M_{ab} = \{0, \kappa^1_{ab}, \kappa^1_{ab}+\kappa^2_{ab}\}$ and $N_{ab} = \{\gamma_{ab}\}$. In order to allow AbrB to repress its own synthesis during vegetative growth [82], we have the constraint $(\kappa^1_{ab}+\kappa^2_{ab})/\gamma_{ab} > \theta^2_{ab}$. The increase of Spo0A~P at the onset of stationary phase shuts off transcription from P2 and induces expression of the AbrB-regulated genes. This yields the constraint $\kappa^1_{ab}/\gamma_{ab} < \theta^1_{ab}$. In summary, we have the equilibrium inequalities

$$0 < \frac{\kappa^1_{ab}}{\gamma_{ab}} < \theta^1_{ab}, \quad \theta^2_{ab} < \frac{\kappa^1_{ab} + \kappa^2_{ab}}{\gamma_{ab}} < max_{ab}. \tag{33}$$

The genes *sinR* (*sin*) and *sinI* (*isin*) are grouped together in the *sin* operon [22, 23, 24]. As shown in figure 3, the operon structure is rather complex: *sinR* is expressed from a σ^A-dependent promoter located between the two coding regions (P3), while both *sinR* and *sinI* are expressed from another σ^A-dependent promoter (P1) preceding the two coding regions [70, 72].[4] Transcription from the latter promoter is activated by Spo0A~P [22, 79] and repressed by AbrB [78], Hpr [38], and presumably SinR [70, 73]. Because a low level of SinI is observed during exponential growth, P1 also seems to allow some constitutive expression of the *sin* operon. Constitutive expression of *sinR* from P1 and P3 leads to a rate of synthesis κ^0_{sr}, while regulated expression from P1 gives rise to a rate of synthesis κ^1_{sr}. With a degradation rate equal to $\gamma_{sr}\, x_{sr}$, we obtain the following state equation for SinR:

$$\begin{aligned}\dot{x}_{sr} = \kappa^0_{sr}\, s^+(x_a,\theta_a) + \kappa^1_{sr}\, s^+(x_a,\theta_a)\, s^-(x_{ab},\theta^1_{ab})\, s^-(x_{hr},\theta_{hr})\,(1 - s^+(x_{sr},\theta^2_{sr})\, s^-(x_{si},\theta^1_{si}))\cdot \\ (1 - s^+(u_s,\theta_s)\, s^+(x_{sa},\theta^2_{sa})\, s^+(x_{ka},\theta^2_{ka})\, s^-(x_{se},\theta^3_{se})) - \gamma_{sr}\, x_{sr}.\end{aligned} \tag{34}$$

The state equation for SinI is similar, with κ^0_{si} denoting the background synthesis rate during exponential growth, κ^1_{si} the synthesis rate induced by derepression of promoter P1 at the onset of stationary phase, and $\gamma_{si}\, x_{si}$ the degradation rate.

[4]The *sin* operon is also transcribed from a third promoter (P2) located between P1 and the *sinI* coding region [72]. P2 has the characteristics of a σ^E-dependent promoter. Because transcription from P2 does not commence but well after the initiation of sporulation, we will omit this promoter here.

$$\dot{x}_{si} = \kappa^0_{si}\, s^+(x_a,\theta_a) + \kappa^1_{si}\, s^+(x_a,\theta_a)\, s^-(x_{ab},\theta^1_{ab})\, s^-(x_{hr},\theta_{hr})\, (1 - s^+(x_{sr},\theta^2_{sr})\, s^-(x_{si},\theta^1_{si}))\cdot$$
$$(1 - s^+(u_s,\theta_s)\, s^+(x_{sa},\theta^2_{sa})\, s^+(x_{ka},\theta^2_{ka})\, s^-(x_{se},\theta^3_{se})) - \gamma_{si}\, x_{si}. \quad (35)$$

SinR represses the expression of various genes involved in the activation of sporulation, such as *spo0A* and *sigF*. In the absence of indications of the contrary, we assume that SinR interacts with these genes at about the same strength. Furthermore, as mentioned above, at higher concentrations SinR must be able to shut off its own synthesis. As explained in section 4.2, this leads to two threshold concentrations for total SinR and SinI, denoted by θ^1_{sr}, θ^2_{sr} and θ^1_{si}, θ^2_{si}, respectively. We obtain the following threshold inequalities

$$0 < \theta^1_{sr} < \theta^2_{sr} < max_{sr}, \quad (36)$$
$$0 < \theta^1_{si} < \theta^2_{si} < max_{si}. \quad (37)$$

As can be verified in (22), a sufficient condition for inhibiting the onset of sporulation is that the concentration of total SinR be above the threshold θ^1_{sr}, while the concentration of total SinI be below the threshold θ^2_{si}.

Inspection of (34) learns that the possible synthesis and degradation rates of SinR are $M_{sr} = \{0, \kappa^0_{sr}, \kappa^0_{sr} + \kappa^1_{sr}\}$ and $N_{sr} = \{\gamma_{sr}\}$. In the exponential growth phase, when SinI is available at low levels, SinR inhibits sporulation [51]. Moreover, SinR autoregulation seems to occur in *sinI* mutants [23, 52]. These conditions imply $\kappa^0_{sr}/\gamma_{sr} > \theta^2_{sr}$, and hence $(\kappa^0_{sr} + \kappa^1_{sr})/\gamma_{sr} > \theta^2_{sr}$. For SinI, we have $M_{si} = \{0, \kappa^0_{si}, \kappa^0_{si} + \kappa^1_{si}\}$ and $N_{si} = \{\gamma_{si}\}$. In wild-type bacteria, SinI seems to prevent free SinR from accumulating to the point where it represses its own synthesis. By means of (34), we conclude that $\kappa^0_{si}/\gamma_{si} > \theta^1_{si}$. Following upregulation of P1, SinI accumulates to the point where it allows derepression of SinR-controlled genes to occur [3]. This motivates the further constraint $(\kappa^0_{si} + \kappa^1_{si})/\gamma_{si} > \theta^2_{si}$. We thus arrive at the following equilibrium inequalities for SinR and SinI

$$\theta^2_{sr} < \frac{\kappa^0_{sr}}{\gamma_{sr}} < max_{sr}, \quad \theta^2_{sr} < \frac{\kappa^0_{sr} + \kappa^1_{sr}}{\gamma_{sr}} < max_{sr}, \quad (38)$$
$$\theta^1_{si} < \frac{\kappa^0_{si}}{\gamma_{si}} < \theta^2_{si}, \quad \theta^2_{si} < \frac{\kappa^0_{si} + \kappa^1_{si}}{\gamma_{si}} < max_{si}. \quad (39)$$

Hpr is a DNA-binding protein regulating the expression of several genes involved in transition state functions of *B. subtilis* [72, 79, 80]. It is the product of the gene *hpr* (*scoC*, *catA*), which is expressed during vegetative growth [38, 60]. Transcription of the gene is repressed by Spo0A∼P [60] and activated by AbrB [81]. Denoting the Hpr concentration by x_{hr}, we obtain the state equation

$$\dot{x}_{hr} = \kappa_{hr}\, s^+(x_a,\theta_a)\, s^+(x_{ab},\theta^1_{ab})\, s^+(u_s,\theta_s)\, s^+(x_{sa},\theta^2_{sa})\, s^+(x_{ka},\theta^2_{ka})\, s^-(x_{se},\theta^3_{se}) - \gamma_{hr}\, x_{hr}, \quad (40)$$

where κ_{hr} and γ_{hr} are synthesis and degradation rate constants, respectively.

Hpr has a single threshold θ_{hr}, which gives the threshold inequalities

$$0 < \theta_{hr} < max_{hr}. \quad (41)$$

Above its threshold, Hpr is able to repress the P1 promoter of the *sin* operon, and thus prevent inactivation of SinR by SinI [38]. Given $M_{hr} = \{0, \kappa_{hr}\}$ and $N_{hr} = \{\gamma_{hr}\}$, this leads to the constraint $\kappa_{hr}/\gamma_{hr} > \theta_{hr}$, and hence the equilibrium inequalities

$$\theta_{hr} < \frac{\kappa_{hr}}{\gamma_{hr}} < max_{hr}. \quad (42)$$

5.6 Sporulation signal

The phosphorelay integrates a variety of environmental and physiological signals, indicating nutrient availibility and cell density [4, 28, 35]. As explained in section 2, we consider a single signal in our model: the signal stimulating the autophosphorylation of the kinases, abbreviated to Signal. It is associated with the input variable u_s, and

$$\dot{u}_s = 0. \tag{43}$$

We define a single threshold for Signal, θ_s, and thus obtain the threshold inequalities

$$0 < \theta_s < max_s. \tag{44}$$

If the step function expression $s^+(u_s, \theta_s)$ evaluates to 1(0), then Signal is said to be present (absent). The presence of Signal denotes physiological conditions conducive to sporulation.

6 Simulation of the sporulation network

The model presented in the previous section consists of 9 state variables, 2 input variables, 22 threshold parameters, and 26 rate parameters. In addition, we specified 70 threshold and equilibrium inequalities. The choice for particular regulation functions and parameter inequalities was motivated by the available genetic and molecular data on *B. subtilis* sporulation. Using this model, we simulate the response of the bacterium to nutrient depletion and high population density for various initial conditions and genetic backgrounds. The leads to qualitative behavioral predictions that can be compared with experimental observations reported in the literature. All simulations reported below have been carried out by means of the program GNA [10].[5]

We will focus on two issues in particular. First, the choice between vegetative growth and sporulation in response to adverse environmental conditions will be explained as the outcome of competing positive and negative feedback loops, controlling the accumulation of Spo0A∼P (section 6.1). Second, the effects of mutation and overexpression on the feedback regulation of Spo0A∼P accumulation will be analyzed (section 6.2).

6.1 Feedback regulation of choice between vegetative growth and sporulation

In response to changing nutrient conditions and population density, *B. subtilis* genes either assume the correct level of activity for sporulation or remain at a level of activity appropriate for vegetative growth [7]. The decision to initiate spore formation or pursue vegetative growth is the result of the integration of signals reflecting the cellular and environmental conditions. On the molecular level, signal integration is accomplished by regulating the activity of the phosphorelay, and hence the accumulation of Spo0A∼P, through positive and negative feedback loops regulating the synthesis of the phosphorelay components [4, 28, 35] (section 2).

[5] The models used for the simulations reported in this section can be obtained from the authors.

In the absence of Signal ($0 \leq u_s < \theta_s$), the system reaches a qualitative equilibrium state associated with the switching domain

$$\begin{array}{ll} \theta_a < u_a \leq max_a, & 0 \leq x_h < \theta_h, \\ 0 \leq x_f < \theta_f, & \theta^1_{sa} < x_{sa} < \theta^2_{sa}, \\ 0 \leq x_{se} < \theta^1_{se}, & \theta^1_{ka} < x_{ka} < \theta^2_{ka}, \\ \theta^1_{hr} < x_{hr} \leq max_{hr}, & x_{ab} = \theta^2_{ab}, \\ \theta^2_{sr} < x_{sr} \leq max_{sr}, & \theta^1_{si} < x^1_{si} < \theta^2_{si}, \\ 0 \leq u_s < \theta_s, & \end{array} \tag{45}$$

which describes physiological conditions found in the exponential growth phase. σ^A is the major sigma factor directing transcription in a vegetatively-growing cell, while σ^H is found at concentrations too low to permit expression of the sporulation genes. The phosphorelay proteins Spo0A and KinA are available at background levels and allow the cell to produce enough Spo0A∼P to enter the transition state if the environmental conditions deteriorate. The transition state regulators SinR, AbrB, and Hpr are available at concentrations preventing the onset of sporulation, while SinI is available at a level that does not permit repression by SinR to be relieved. The gene coding for σ^F is not expressed in a growing cell.

Starting from this qualitative equilibrium state, we perturb the system by switching on the sporulation signal ($\theta_s < u_s \leq max_s$). Simulation of the network takes a few seconds to complete on a PC (500 MHz, 128 MB), and gives rise to a transition graph of 465 qualitative states. Many of these states are associated with switching domains that the system traverses instantaneously. Since the biological relevance of the latter states is limited, they can be eliminated from the transition graph. This leads to a reduced transition graph of 82 qualitative states, part of which is shown in figure 12.

The transition graph contains a single qualitative equilibrium state that the system eventually reaches in all qualitative behaviors. The qualitative equilibrium state corresponds to the *spo*$^-$ phenotype, because the concentration of σ^F has not reached the threshold above which it directs the transcription of its target genes. Whereas in some qualitative behaviors the system directly reaches the qualitative equilibrium state, in others it first passes through a period of transitory *sigF* expression, which corresponds to the *spo*$^+$ phenotype.

Typical qualitative behaviors for sporulation as well as for vegetative growth are explored in detail in figure 12. The first event after receiving the sporulation signal is the downregulation of *abrB*, which favors expression of *sigH* and *sinI*. Expression of *sinI* is further stimulated by the disappearance of Hpr, whose synthesis is shut off following *abrB* downregulation. Increasing levels of σ^H and SinI lead to an increase in *spo0A* and *kinA* expression. As a consequence, Spo0A∼P levels continue to rise and eventually activate *sigF* expression (figure 12(b)). On the other hand, *abrB* downregulation also causes the Spo0E concentration to rise, which prevents Spo0A∼P from accumulating to the point where *sinI* is expressed at a level sufficient to inactivate SinR. This leaves SinR repression of the σ^H-dependent promoter of Spo0A intact, and thus prevents activation of *sigF* expression (figure 12(c)).

We conclude that the transition graph faithfully represents the two possible responses to nutrient depletion that are observed for *B. subtilis*: either the bacterium continues vegetative growth or it enters sporulation. The initiation of sporulation is determined by positive feedback loops acting through Spo0A and KinA, and a negative feedback loop involving Spo0E. When the rate of accumulation of the kinase outpaces the rate of accumulation of the phosphatase, we observe transient expression of *sigF*, *i.e.* a *spo*$^+$ phenotype (figure 12(b)). If the kinetics of these processes are inversed, *sigF* is never activated and we observe a *spo*$^-$ phenotype (figure 12(c)). Additional negative feedback loops stabilize the expression of *spo0A* and *kinA* at high concentrations of Spo0A∼P.

The expression of *sigF* in the sporulation behavior is transitory. The reversion of the sporulation decision, caused by the continuing accumulation of Spo0E, is due to the fact that the genes and

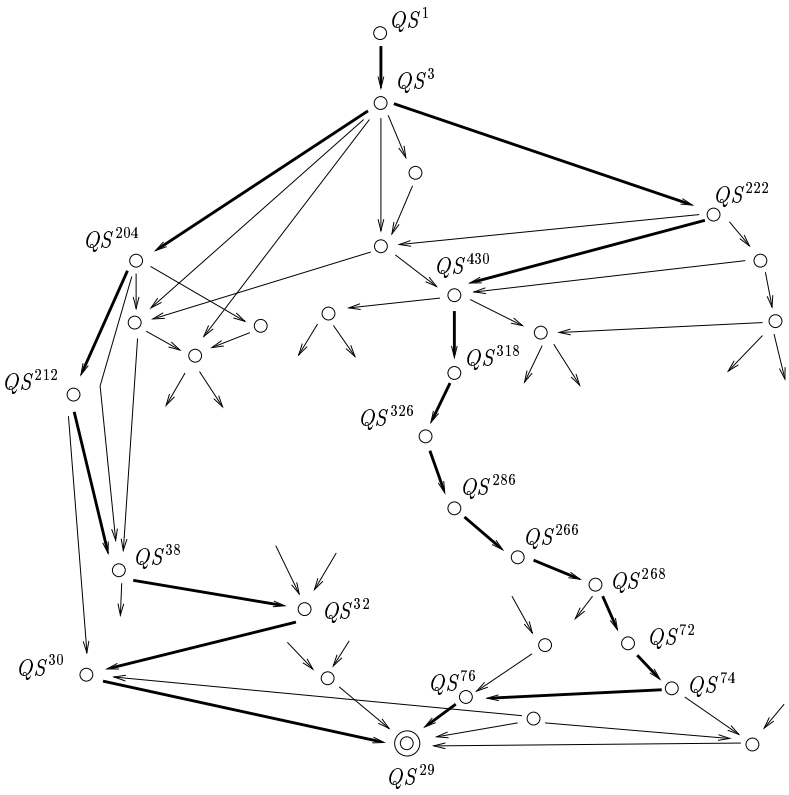

(a)

Figure 12: (a) Fragment of the state transition graph produced for vegetative growth conditions, when Signal is switched on ($\theta_s < u_s \leq max_s$). (b) Temporal evolution of selected protein concentrations in a typical qualitative behavior leading to the spo^+ phenotype. (c) Idem, but for a typical qualitative behavior leading to the spo^- phenotype.

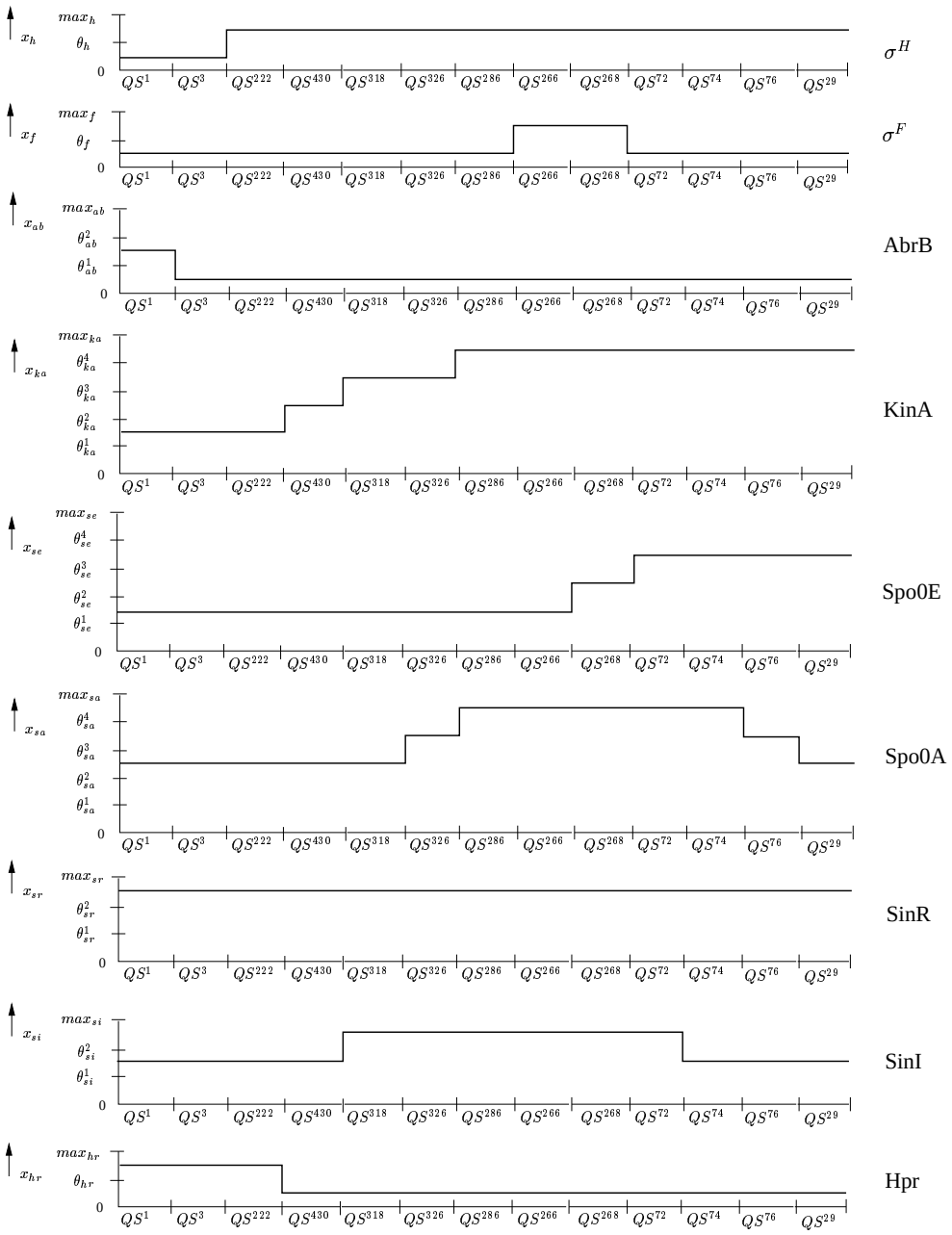

(b)

Figure 12: Continued.

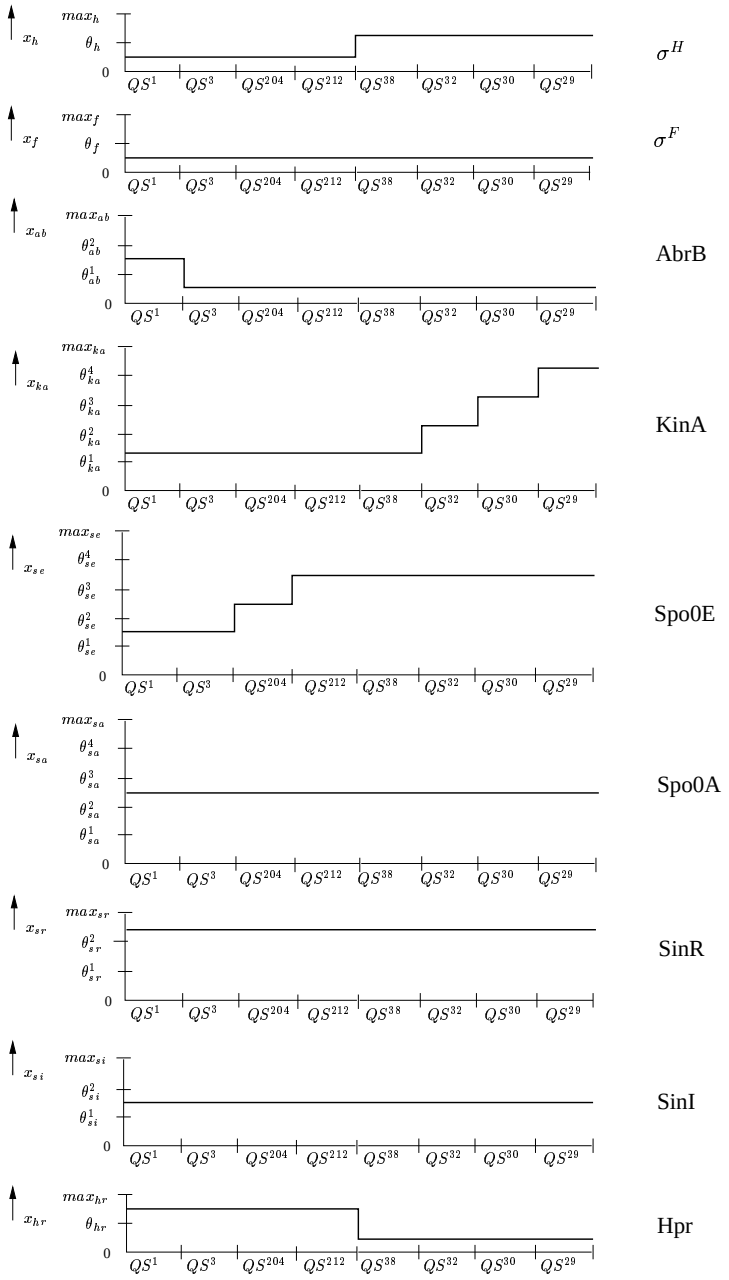

(c)

Figure 12: Continued.

interactions required for later stages of sporulation, as well as signalling mechanisms controlling the activation of the kinases and phosphatases, have not been included in our model. In section 7, we discuss how the model could be extended to include these processes.

6.2 Feedback regulation in different genetic backgrounds

Much of our knowledge on the architecture of the network in figure 3 derives from studies describing the effects of mutation and overexpression of sporulation genes. Changing the genetic background amounts to disrupting the network structure, *e.g.*, deleting a gene or removing a regulatory interaction. The genetic modifications disable some of the feedback loops of the system, and may thus influence the choice of developmental pathway. In particular, mutation and overexpression of some genes may lead to qualitatively different outcomes, in the sense that either the spo^+ or the spo^- phenotype disappears.

From the literature, we have selected a dozen genetic modifications concerning most of the genes in the reduced sporulation network of figure 3. For each case, table 1 lists the nature of the modification (deletion of the coding region or a promoter of a gene, overexpression of a gene). The genetic modifications are integrated into the model of section 5 by adapting state equations or parameter inequalities, as illustrated in the examples below. The modified strains have been simulated for vegetative growth conditions (45), sometimes slightly modified to account for the difference in genetic background, in the presence of the sporulation signal. The simulation results have been compared with experimental data. A specific sporulation phenotype (spo^+ or spo^-) is said to be observed, if a non-negligible proportion of the culture ($> 1\%$) has this phenotype under the experimental conditions. The simulation results and their correspondence with experimental observations are summarized in the table.

Modification	Reference	States	Predicted phenotype	Correct?
spo0A deletion	[34]	2 (1)	spo^-	Y
spo0A(P_S) disruption	[71]	187 (40)	spo^-	Y
sigH deletion	[34]	17 (7)	spo^-	Y
kinA deletion	[37, 47, 87]	2 (1)	spo^-, spo^+	N
spo0E deletion	[61]	100 (39)	spo^-, spo^+	N
spo0E overexpression	[61]	2 (1)	spo^-	Y
spo0A abrB deletion	[29]	135 (30)	spo^-	Y
sinR deletion	[51]	1257 (142)	spo^-, spo^+	Y
sinR overexpression	[23]	137 (31)	spo^-	Y
kinA sinR deletion	[50, 51]	2 (1)	spo^-, spo^+	N
sinI deletion	[3]	137 (31)	spo^-	Y
hpr overexpression	[60]	47 (16)	spo^-	Y

Table 1: Qualitative simulation of cell in different genetic backgrounds, under physiological conditions corresponding to vegetative growth, in the presence of the sporulation signal. The number of qualitative states generated, as well as the predicted sporulation phenotype (spo^- or spo^+), are listed. In addition, it is indicated whether the qualitative behaviors predicted by the model are consistent (Yes or No) with the observations.

For example, deletion of the gene *sigH* means that the sigma factor σ^H cannot be synthesized. In order to model the behavior of this mutant, we change (16), the state equation for σ^H, into

$$\dot{x}_h = -\gamma_h \, x_h, \tag{46}$$

which reflects that a *sigH* mutant is not able to produce any σ^H. Qualitative simulation using the model thus modified results in a state transition graph with a single qualitative equilibrium state, corresponding to the spo^- phenotype (figure 13). No expression, not even transitory, of the gene *sigF* occurs. As can be seen in (b), *abrB* downregulation still occurs, leading to activation of *spo0E* and

repression of *hpr*, but the concentration of σ^H-dependent sporulation genes remains below the thresholds necessary for the initiation of sporulation. The disappearance of the *spo*$^+$ phenotype corresponds exactly to the observed biological behavior: a *sigH* mutant does not sporulate [34].

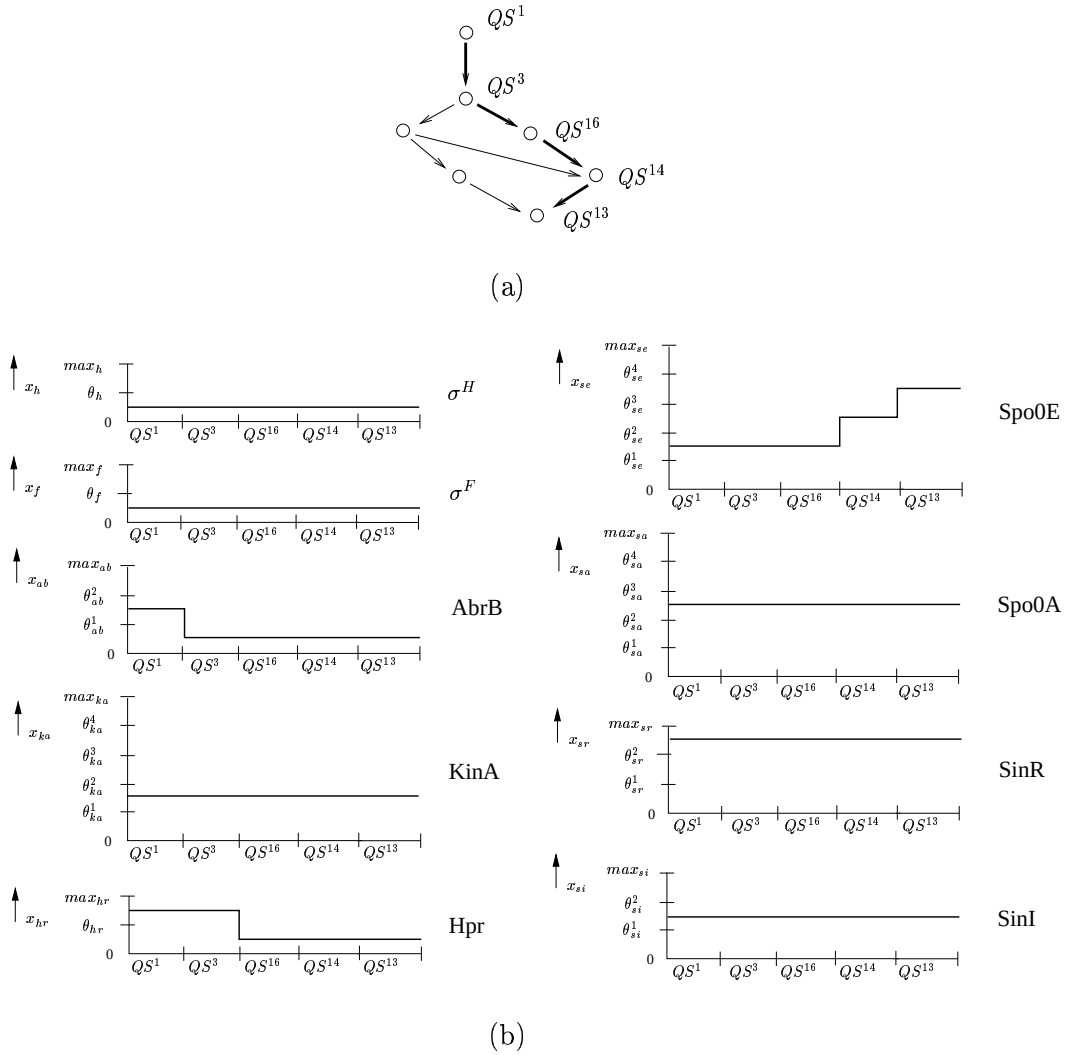

Figure 13: (a) Fragment of the state transition graph produced for vegetative growth conditions in a *sigH* mutant, when Signal is present ($\theta_s < u_s \leq max_s$). (b) Temporal evolution of the proteins in a typical qualitative behavior.

Disruption of the P_S promoter of *spo0A* also inhibits sporulation [71]. The state equation of Spo0A changes into

$$\dot{x}_{sa} = \kappa^1_{sa}\, s^+(x_a, \theta_a)\,(1 - s^+(u_s, \theta_s)\, s^+(x_{sa}, \theta^3_{sa})\, s^+(x_{ka}, \theta^3_{ka})\, s^-(x_{se}, \theta^2_{se})) - \gamma_{sa}\, x_{sa}. \qquad (47)$$

In comparison with (22), the term involving κ^2_{sa}, the rate of synthesis of Spo0A from P_S transcripts, has been omitted. Qualitative simulation yields a state transition graph with 187 states (40 of which are non-instantaneous), containing a single qualitative equilibrium state that corresponds to the *spo*$^-$ phenotype. Contrary to what is observed in the case of the *sigH* mutant, an increase of KinA synthesis occurs at the onset of stationary phase, due to derepression of *sigH*.

Overexpression of *spo0E* renders strains incapable of sporulation [61]. The negative feedback loop is disrupted, because Spo0E is continuously available at high concentrations, thus washing away the effects of AbrB regulation. This can be modeled by changing the equilibrium inequalities for Spo0E into

$$\theta^4_{se} < \frac{\kappa^0_{se}}{\gamma_{se}} < max_{se}, \quad \theta^4_{se} < \frac{\kappa^0_{se} + \kappa^1_{se}}{\gamma_{se}} < max_{se}. \tag{48}$$

Qualitative simulation confirms that sporulation cannot be initiated under these conditions.

Overall, we find good correspondence between the observed and predicted qualitative behavior of genetically modified strains under sporulation conditions. However, simulation of the cell in a *kinA* background gives rise to a transition graph without a qualitative behavior corresponding to the *spo*$^+$ phenotype. This prediction is in contradiction with the observation that deletion of *kinA* does not substantially diminish the capability of the bacterium to sporulate, although the onset of sporulation is delayed [37, 47, 87]. The incorrect prediction results from ignoring additional kinases that play a role in the initiation of sporulation, in particular KinB and KinC [37, 41, 46, 47, 87]. For a similar reason, omitting alternative kinases or phosphatases, the model fails to correctly predict the behavior of the *kinA sinR* and the *spo0E* mutants. Extension of the sporulation model with state equations for the alternative kinases and phosphatases restores the capacity of the model to account for the *kinA* and *spo0E* mutants (results not shown).

7 Discussion

In this report, we have modeled and simulated the genetic regulatory network underlying the decision between vegetative growth and sporulation in the Gram positive soil bacterium *B. subtilis*. We have used the qualitative simulation method described in [10], which is based on a class of PL differential equation models. The PL models describe a genetic regulatory network as a set of genes encoding proteins that control the synthesis and degradation of other proteins. The models abstract from the precise molecular mechanisms involved in the regulation of gene expression and proteolysis, such as the interactions in the phosphorelay. Instead, they employ step functions capturing essential aspects of the regulatory logic of the mechanisms. The PL models are particularly appropriate for a global description of the sporulation process, which can be understood as a switch between genetic programs, involving a change in expression of a large number of genes. For other purposes, for instance when focusing on a specific molecular mechanism, more fine-grained models may be required [8].

The step functions in the PL models are approximations of sigmoidal functions expressing the relation between the concentration of a regulatory protein and the activity of a target gene [66, 95]. The sigmoidal form of regulation functions arises from cooperative effects, such as the multimerization of regulatory proteins and the existence of several binding sites for a protein in the promoter region of the target gene. Since many of the regulatory proteins in the sporulation network are active as multimers, *e.g.*, SinR [24], Spo0A [49], and AbrB [88], the assumption of sigmoidal regulation functions seems warranted. A novelty of our work is that is shows that the activity of a gene as a function of the concentration of several proteins, involved in a complex regulatory mechanism, may give rise to a multi-dimensional sigmoidal curve. When building a detailed kinetic model of the molecular interactions, and simplifying the model by means of the quasi-equilibrium assumption, generalized sigmoidal functions are found for the regulatory mechanisms involving SinR and Spo0A$\sim$P (section 4).

Instead of assigning numerical values to the threshold and rate parameters, we specify qualitative constraints on the parameters in the form of algebraic inequalities. This results in a qualitative model of the sporulation network (figure 11). The use of qualitative models is motivated by the fact that, even though sporulation in *B. subtilis* is one of the best-understood model systems for prokaryotic development, very little quantitative data on kinetic parameters and molecular concentrations are available. This compromises the use of traditional numerical methods, especially when the size of the sporulation model (11 variables and 48 parameters) is taken into account. Whereas numerical values for the parameters are absent, the discussion of the model in section 5 shows that information required for the choice of appropriate threshold and equilibrium inequalities can be derived from the experimental literature.

The parameter inequalities are exploited by the simulator GNA which, based on the mathematical properties of the PL models, predicts the possible qualitative behaviors of the system. More precisely, the program generates a state transition graph consisting of qualitative states and transitions between qualitative states. A path in the state transition graph corresponds to a predicted qualitative behavior of the system, describing the qualitative evolution of protein concentrations over time. The graphical interface module of GNA offers visualization functions to analyze the predicted qualitative behaviors in detail (figure 12).

The predictions obtained through qualitative simulation are less precise than their numerical counterparts. We can predict that, under conditions of nutrient deprivation, the KinA and Spo0E concentrations will increase over time. However, we cannot predict the numerical value to which the concentrations will rise. In addition, while a strain bearing a *sinR* deletion is correctly predicted to have the spo^+ and spo^- phenotypes, it is not possible to conclude from the transition graph that the mutant strain sporulates more frequently than the wild-type strain, nor that *sigF* is expressed earlier in a *sinR* background [51]. Although the qualitative behaviors lack numerical precision, they do nevertheless capture essential features of the dynamics of the regulatory system.

In the case of the response of *B. subtilis* to nutrient deprivation, two kinds of qualitative behavior are found, in accordance with the observations (section 6.1): one type of behavior corresponds to the initiation of sporulation (spo^+), whereas the other signifies a continuation of vegetative growth (spo^-) (figure 12). The spo^+ phenotype arises from the (transient) expression of *sigF*, whereas in the spo^- phenotype *sigF* is not expressed at all. Given the qualitative description of the network of interactions and the sporulation conditions, these are the only possible responses of the system. This follows from the soundness of the qualitative simulation method, which guarantees that all qualitative behaviors abstracting from some solution of a quantitative PL model, consistent with the qualitative PL model, are covered by the state transition graph (section 3). Notice that this guarantee is obtained without performing exhaustive numerical simulation.

The decision to enter sporulation or pursue vegetative growth emerges from the complex network of interactions in figure 11. The key determinant of the behavior of the cell is the transcriptional regulation of the phosphorelay proteins Spo0A, KinA, and Spo0E achieved by a number of competing positive and negative feedback loops. The feedback loops ensure that small external stimuli, such as the signal causing autophosphorylation of KinA, can be amplified and provoke a dramatic change in the overall pattern of gene activity. Figure 12(b) describes the situation in which the positive feedback loops act stronger than the negative feedback loop. In this case, the accumulation of KinA outpaces the accumulation of Spo0E, and the concentration of Spo0A reaches a level at which sporulation can be initiated. In figure 12(c), the concentration of Spo0E rises faster than the concentration of KinA, and SinI cannot reach the threshold concentration above which it is able to neutralize SinR. The sequences of events predicted by the qualitative behaviors correspond well to the observed qualitative changes in gene expression.

The same design principle of competing feedback loops is found in the genetic network controlling the lysis-lysogeny decision of bacteriophage λ [66]. Here, the feedback loops install a race between the activator protein CI and the repressor protein Cro, analogously to the competition between KinA and Spo0E in the sporulation network. Such a design possesses 'undesirable' properties from an engineering point of view, because of its extreme sensitivity to small variations in the environmental conditions. However, networks based on this principle appear to be quite appropriate for biological decision-making involving the integration of a variety of heterogeneous signals (see [85] for a general account of the role of feedback loops in development). As in the case of sporulation, mutation of the genes involved in the lysis-lysogeny decision affect the ability of the system to weigh and integrate a variety of possibly contradictory signals.

The signal integration mechanism controlling the initiation of sporulation in *B. subtilis* is actually even more complex than shown in figures 3 and 4. As explained in section 2, the phosphorelay transfers a phosphate from the kinase to Spo0A in multiple steps, each of which may be separately controlled

by environmental and physiological signals. In addition, multiple kinases and phosphatases have been shown to play a role in the sporulation decisions, whereas we have taken into account a single kinase and phosphatase. Recent work has shown that some mechanisms transducing signals relevant for the sporulation decision involve proteins inhibiting the activity of the kinases and phosphatases [45, 89]. Since these regulatory proteins are, in some instances at least, under the direct or indirect control of Spo0A∼P, this gives rise to an additional layer of feedback control of the phosphorelay. We are currently working on extended models of the sporulation network, taking into account the above interactions as well as interactions involved in later stages of the sporulation process.

One of the alternative phosphatases in the phosphorelay, RapA, is under the control of ComA∼P, a response regulator involved in genetic competence [56]. This brings to the fore that the binary decision between vegetative growth and sporulation is a simplification. In fact, as mentioned in the introduction, the behavioral repertoire of *B. subtilis* includes other, less drastic responses to degrading environmental conditions. Among these is the development of genetic competence, that is, the uptake of foreign DNA and its integration into the genome of the bacterium [13, 28]. In this report, we have investigated a single module, responsible for the decision to initiate sporulation. But in reality this module interacts with other modules, regulating the development of competence and motility, the production of antibiotics, and other responses. We plan to address the interactions between these modules in extended models of the stationary-phase behavior of *B. subtilis*.

The initiation of sporulation is one of the best-studied examples of development in prokaryotes. This has allowed us to compile from published sources a detailed model of the genetic regulatory network controlling this process. The coherence between the model predictions and the observed biological behaviors can be seen as a validation of the modeling and simulation approach that we have chosen, which is based on coarse-grained and qualitative models of regulatory networks. The results from this study, and from studies carried out with logical models related to the PL models used in this paper [53, 67, 84], warrant the future application of the method to biological systems that are understood to a lesser degree. The possibility to explore alternative hypotheses of the network structure through qualitative simulation may guide the choice of discriminatory experiments and thus contribute to the efficient mapping of genetic regulatory networks.

A Kinetic models of regulatory mechanisms

A.1 Transcription regulator

Consider the regulation of *hpr* by AbrB in figure 5(a). Using the mass-action rate law, a detailed mechanistic model of the interaction could be developed, possibly taking into account dimerization of the regulatory protein and the presence of multiple binding sites in the promoter region of the gene (*e.g.*, [1, 40, 92]). For our purposes, it will suffice to use the Hill rate law, a simpler, phenomenological relation between the activity of a gene and the concentration of a transcriptional regulator [25, 33, 85]. Denoting by ν_{hr} the normalized activity of gene *hpr*, $0 \leq \nu_{hr} \leq 1$, and by x_{ab} the concentration of AbrB, the Hill function is defined as

$$\nu_{hr} = \frac{x_{ab}^{\sigma}}{x_{ab}^{\sigma} + K_{ab}^{\sigma}},$$

where $\sigma > 1$ is the cooperativity coefficient and $K_{ab} > 0$ a phenomenological constant analogous to the half-saturation constant in Michealis-Menten kinetics. The Hill function has a sigmoid shape, which corresponds to experimental observations of bacterial gene regulation [66, 95]. K_{ab} can be interpreted as a measure of the strength of the interaction between the regulatory protein AbrB and the promoter region of *hpr*.

For arbitrary but realistic parameter values, we obtain the gene activity plots in figure 6 ($K_{ab} = 5 \cdot 10^{-6}$ M and $\sigma = 3$ in (a); $K_{ab} = 6.7 \cdot 10^{-6}$ M and $\sigma = 3$ in (b)). All calculations and plots have been produced using the program Matlab (MathWorks).

A.2 Transcription regulator inactivated by anti-repressor

The regulation of *spo0A* in figure 7 can be modeled by means of the mass-action and the Hill rate laws. Let ν_{sa} and K_{sr} be defined analogously to ν_{hr} and K_{ab} in appendix A.1. The activity of *spo0A* as a function of the free SinR concentration $x_{sr\sim}$ is then given by the algebraic equation

$$\nu_{sa} = 1 - \frac{x_{sr\sim}^{\sigma}}{x_{sr\sim}^{\sigma} + K_{sr}^{\sigma}} = \frac{K_{sr}^{\sigma}}{x_{sr\sim}^{\sigma} + K_{sr}^{\sigma}}. \tag{49}$$

The following reactions are involved in the association of SinI and SinR, and the dissociation of the SinR∼SinI complex:

$$\text{SinR} + \text{SinI} \underset{k_{-1}}{\overset{k_1}{\rightleftarrows}} \text{SinR}\sim\text{SinI}$$

k_1 and k_{-1} are the rate constants for the association and dissociation step, respectively. The reactions are described by the system of differential equations

$$\dot{x}_{sr\sim} = k_{-1}\, x_{sr\sim si} - k_1\, x_{sr\sim}\, x_{si\sim}, \tag{50}$$

$$\dot{x}_{si\sim} = k_{-1}\, x_{sr\sim si} - k_1\, x_{sr\sim}\, x_{si\sim}, \tag{51}$$

$$\dot{x}_{sr\sim si} = k_1\, x_{sr\sim}\, x_{si\sim} - k_{-1}\, x_{sr\sim si}, \tag{52}$$

where $x_{si\sim}$ and $x_{sr\sim si}$ denote the concentrations of free SinI and of SinR∼SinI, respectively. In addition, we define the following conservation relations for the total SinR and SinI concentrations x_{sr} and x_{si}:

$$x_{sr} = x_{sr\sim} + x_{sr\sim si}, \tag{53}$$

$$x_{si} = x_{si\sim} + x_{sr\sim si}. \tag{54}$$

The conservation relations (53)-(54) allow the system (50)-(52) to be simplified to the single differential equation:

$$(1/k_1)\, \dot{x}_{sr\sim} = -x_{sr\sim}^2 + (x_{sr} - x_{si} - K_1)\, x_{sr\sim} + K_1\, x_{sr}, \tag{55}$$

where $K_1 = k_{-1}/k_1$. (49) and (55) together describe the regulatory mechanism in figure 7.

Following the quasi-equilibrium assumption in section 4.2, we set $\dot{x}_{sr\sim} = 0$. The equilibrium concentration of $x_{sr\sim}$ can be obtained by finding the roots of the second-order polynomial in the right-hand side of (55). The polynomial has two roots, but a simple argument shows that only one root lies inside the range $0 \leq x_{sr\sim} \leq x_{sr}$. For $x_{sr\sim} = 0$, the polynomial simplifies to $K_1\, x_{sr}$, whereas for $x_{sr\sim} = x_{sr}$, we obtain $-x_{si}\, x_{sr}$. The first term is positive and the second negative, hence there is a single root in $0 \leq x_{sr\sim} \leq x_{sr}$. Moreover, this root corresponds to an asymptotically stable steady-state of the system, since $\partial \dot{x}_{sr\sim}/\partial x_{sr\sim} < 0$. (In fact, $\partial \dot{x}_{sr\sim}/\partial x_{sr\sim} = -2k_1\, x_{sr\sim} + k_1\, x_{sr} - k_1\, x_{si} - k_{-1} = -k_1\, x_{sr\sim} - k_1\, x_{si\sim} - k_{-1} < 0$.)

Taking arbitrary, but realistic values for the parameters ($K_1 = 800 \cdot 10^3$ M, $K_{sr} = 0.2 \cdot 10^{-6}$ M, $\sigma = 3$), we have calculated the valid root of the polynomial in (55), for different concentrations of total SinR and SinI. This yields the concentration of free SinR at equilibrium, and hence the activity plot of *spo0A* shown in figure 8. The result is robust, in the sense that moderate variations in the parameter values do not change the sigmoidal shape of the surface. The activity plot for the regulation of *sinR* is obtained in the same way, with $K_1 = 800 \cdot 10^3$ M, $K_{sr} = 0.4 \cdot 10^{-6}$ M, and $\sigma = 3$.

A.3 Transcription regulator phosphorylated through phosphorelay

The activation of the expression of *sigF* by Spo0A∼P (figure 9) is described by means of the Hill rate law

$$\nu_f = \frac{x^{\sigma}_{sa\sim p}}{x^{\sigma}_{sa\sim p} + K^{\sigma}_{sa}}, \tag{56}$$

where $x_{sa\sim p}$ and ν_f denote the concentration of Spo0A∼P and the normalized activity of *sigF*, respectively, while the constants K_{sa} and σ have their usual meaning.

The reduced phosphorelay of figure 9 then involves the following reactions and rate constants:

$$\begin{array}{ccccc}
\text{Spo0A} + \text{KinA} & \underset{k_{-1}}{\overset{k_1}{\rightleftarrows}} & \text{Spo0A} \sim \text{KinA} & \xrightarrow{k_2} & \text{Spo0A} \sim \text{P} + \text{KinA} \\
\text{Spo0A}\sim\text{P} + \text{Spo0E} & \underset{k_{-3}}{\overset{k_3}{\rightleftarrows}} & \text{Spo0A} \sim \text{Spo0E} & \xrightarrow{k_4} & \text{Spo0A} + \text{Spo0E}
\end{array}$$

Recall from section 2 that the autophosphorylation of KinA is stimulated by a sporulation signal, the molecular nature of which has escaped experimental identification thus far.

The reactions are modeled by means of the law of mass action (see [69] for a similar model). Let $x_{sa\sim p}$, $x_{sa\sim}$ denote the phosphorylated and non-phosphorylated Spo0A concentrations, $x_{ka\sim}$, $x_{se\sim}$ the free KinA, Spo0E concentrations, and $x_{sa\sim ka}$, $x_{sa\sim se}$ the Spo0A∼KinA, Spo0A∼Spo0E concentrations. Then we obtain the following system of differential equations:

$$\dot{x}_{sa\sim} = k_{-1}\, x_{sa\sim ka} + k_4\, x_{sa\sim se} - k_1\, x_{sa\sim}\, x_{ka\sim}, \tag{57}$$
$$\dot{x}_{sa\sim p} = k_{-3}\, x_{sa\sim se} + k_2\, x_{sa\sim ka} - k_3\, x_{sa\sim p}\, x_{se\sim}, \tag{58}$$
$$\dot{x}_{sa\sim ka} = k_1\, x_{sa\sim}\, x_{ka\sim} - (k_{-1} + k_2)\, x_{sa\sim ka}, \tag{59}$$
$$\dot{x}_{sa\sim se} = k_3\, x_{sa\sim p}\, x_{se\sim} - (k_{-3} + k_4)\, x_{sa\sim se}, \tag{60}$$
$$\dot{x}_{ka\sim} = (k_{-1} + k_2)\, x_{sa\sim ka} - k_1\, x_{sa\sim}\, x_{ka\sim}, \tag{61}$$
$$\dot{x}_{se\sim} = (k_{-3} + k_4)\, x_{sa\sim se} - k_3\, x_{sa\sim p}\, x_{se\sim}. \tag{62}$$

In addition, we define the following conservation relations:

$$x_{ka} = x_{ka\sim} + x_{sa\sim ka}, \tag{63}$$
$$x_{se} = x_{se\sim} + x_{sa\sim se}, \tag{64}$$
$$x_{sa} = x_{sa\sim} + x_{sa\sim p} + x_{sa\sim ka} + x_{sa\sim se}, \tag{65}$$

where x_{ka}, x_{se}, x_{sa} denote the total KinA, Spo0E, Spo0A concentrations. Thus, following (63), the total kinase concentration equals the sum of its free and complexed concentration (idem for the phosphatase).

We will assume, as in the case of the phosphorylation/dephosphorylation cascade studied by Shacter *et al.* [69], that the amount of enzyme-substrate complex is negligible in comparison with the amount of phosphorylated and non-phosphorylated substrate. As a consequence, we can simplify (65) to $x_{sa} = x_{sa\sim} + x_{sa\sim p}$. We will further assume that the enzyme-catalyzed reactions follow Michaelis-Menten kinetics. This leads to $\dot{x}_{sa\sim ka} = 0$ and $\dot{x}_{sa\sim se} = 0$.

The conservation relations (63)-(65), together with the assumptions detailed in the previous paragraph, allow the rate equations (57)-(62) to be simplified. In the presence of Signal, we obtain the single differential equation

$$\dot{x}_{sa\sim p} = \frac{(k_4\, x_{se} - k_2\, x_{ka})\, x^2_{sa\sim p} - (k_4\, x_{se}\, (K_1 + x_{sa}) + k_2\, x_{ka}\, (K_3 - x_{sa}))\, x_{sa\sim p} + k_2\, K_3\, x_{sa}\, x_{ka}}{(K_1 + (x_{sa} - x_{sa\sim p}))\, (K_3 + x_{sa\sim p})}. \tag{66}$$

where $K_1 = (k_{-1} + k_2)/k_1$ and $K_3 = (k_{-3} + k_4)/k_3$.

In section 4.3, it was argued that the phosphorelay is in a state of quasi-equilibrium with respect to the synthesis and degradation of its component proteins. We therefore set $\dot{x}_{sa\sim p} = 0$ in (66), and solve for $x_{sa\sim p}$. We have to determine the roots of the polynomial on the right-hand side of the equation. By an argument parallel to that given in the previous section, it can be shown that there is a single root in the interval $0 \leq x_{sa\sim} \leq x_{sa}$, which corresponds to an asymptotically stable equilibrium of the system. The gene activity ν_{kb} at equilibrium can then be calculated by means of (56).

The above derivation is valid under the condition that the signal stimulating autophosphorylation of KinA is present. In the absence of Signal, (66) reduces to

$$\dot{x}_{sa\sim p} = 0, \tag{67}$$

and the system is in equilibrium by definition. Since Spo0A is synthesized in its unphosphorylated form, we fix this equilibrium at $x_{sa\sim p} = 0$.

Based on the experimental literature [27], the following approximate parameter values have been chosen: $K_1 = 2.1 \cdot 10^{-6}$ M, $K_3 = 1.5 \cdot 10^{-6}$ M, $k_2 = 0.085$ s^{-1}, and $k_4 = 0.2$ s^{-1}. For the remaining parameters, we have used the values $K_f = 1.8 \cdot 10^{-6}$ M and $\sigma = 3$. Calculation of the activity of *sigF* as a function of the concentrations of Spo0A, KinA, and Spo0E, in the absence and presence of Signal, leads to the plots shown in figure 10. The sigmoidal shape of the surface is robust under moderate variation of the parameter values. The activity plots for the regulation of *abrB* (not shown) are obtained in the same way, with a lower value for K_{kb}.

References

[1] G.K. Ackers, A.D. Johnson, and M.A. Shea. Quantitative model for gene regulation by λ phage repressor. *Proceedings of the National Academy of Sciences of the USA*, 79:1129–1133, 1997.

[2] C. Antoniewski, B. Savelli, and P. Stragier. The *spoIIJ* gene, which regulates early developmental steps in *Bacillus subtilis*, belongs to a class of environmentally responsive genes. *Journal of Bacteriology*, 172(1):86–93, 1990.

[3] U. Bai and I. Mandić-Mulec. SinI modulates the activity of SinR, a developmental switch protein of *Bacillus subtilis*, by protein-protein interaction. *Genes & Development*, 7:139–148, 1993.

[4] D. Burbulys, K.A. Trach, and J.A. Hoch. Initiation of sporulation in *Bacillus subtilis* is controlled by a multicomponent phosphorelay. *Cell*, 64:545–552, 1991.

[5] W.F. Burkholder and A.D. Grossman. Regulation of the initiation of endospore formation in *Bacillus subtilis*. In Y.V. Brun and L.J. Shimkets, editors, *Prokaryotic Development*, chapter 7, pages 151–166. American Society for Microbiology, Washington, DC, 2000.

[6] H.L. Carter 3rd and C.P. Moran, Jr. New RNA polymerase σ factor under *spo0* control in *Bacillus subtilis*. *Proceedings of the National Academy of Sciences of the USA*, 83(24):9438–9442, 1986.

[7] J.D. Chung, G. Stephanopoulos, K. Ireton, and A.D. Grossman. Gene expression in single cells of *Bacillus subtilis*: Evidence that a threshold mechanism controls the initiation of sporulation. *Journal of Bacteriology*, 176(7):1977–1984, 1994.

[8] H. de Jong. Modeling and simulation of genetic regulatory systems: A literature review. *Journal of Computational Biology*, 9(1):69–105, 2002.

[9] H. de Jong, J. Geiselmann, C. Hernandez, and M. Page. Genetic Network Analyzer: A tool for the qualitative simulation of genetic regulatory networks. *Bioinformatics*, 2002. Accepted for publication.

[10] H. de Jong, J.-L. Gouzé, C. Hernandez, M. Page, T. Sari, and H. Geiselmann. Qualitative simulation of genetic regulatory networks using piecewise-linear models. Technical Report RR-4407, INRIA, 2002.

[11] H. de Jong, M. Page, C. Hernandez, and J. Geiselmann. Qualitative simulation of genetic regulatory networks: Method and application. In B. Nebel, editor, *Proceedings of the Seventeenth International Joint Conference on Artificial Intelligence, IJCAI-01*, pages 67–73, San Mateo, CA, 2001. Morgan Kaufmann.

[12] L.G. Dixon, S. Seredick, M. Richer, and G.B. Spiegelman. Developmental gene expression in *Bacillus subtilis crsA47* mutants reveals glucose-activated control of the gene for the minor sigma factor σ^H. *Journal of Bacteriology*, 183(16):4814–4822, 2001.

[13] D. Dubnau and K. Turgay. Regulation of competence in *Bacillus subtilis* and its relation to stress response. In G. Storz and R. Hengge-Aronis, editors, *Bacterial Stress Responses*, chapter 17, pages 249–260. American Society for Microbiology, Washington, DC, 2000.

[14] E. Dubnau, J. Weir, G. Nair, L. Carter 3rd, C.P. Moran, Jr., and I. Smith. *Bacillus* sporulation gene *spo0H* codes for σ^{30} (σ^H). *Journal of Bacteriology*, 170(3):1054–1062, 1988.

[15] J. Errington. Septation and chromosome segregation during sporulation in *Bacillus subtilis*. *Current Opinion in Microbiology*, 4(6):660–666, 2001.

[16] C. Eymann, G. Mittenhuber, and M. Hecker. The stringent response, σ^H-dependent gene expression and sporulation in *Bacillus subtilis*. *Molecular and General Genetics*, 264(1-2):913–923, 2001.

[17] P. Fawcett, P. Eichenberger, R. Losick, and P. Youngman. The trancriptional profile of early to middle sporulation in *Bacillus subtilis*. *Proceedings of the National Academy of Sciences of the USA*, 97(14):8063–8068, 2000.

[18] F.A Ferrari, K. Trach, D. LeCoq, J. Spence, E. Ferrari, and J.A. Hoch. Characterization of the *spo0A* locus and its deduced product. *Proceedings of the National Academy of Sciences of the USA*, 82(9):2647–2651, 1985.

[19] A.F. Filippov. *Differential Equations with Discontinuous Righthand Sides*. Kluwer Academic Publishers, Dordrecht, 1988.

[20] P. Fort and P.J. Piggot. Nucleotide sequence of sporulation locus *spoIIA* in *Bacillus subtilis*. *Journal of General Microbiology*, 130(Pt 8):2147–2153, 1984.

[21] M. Fuyita and Y. Sadaie. Feedback loops involving Spo0A and AbrB in *in vitro* transcription of the genes involved in the initiation of sporulation in *Bacillus subtilis*. *Journal of Biochemistry*, 124:98–104, 1998.

[22] N.K. Gaur, K. Cabane, and I. Smith. Structure and expression of the *Bacillus subtilis sin* operon. *Journal of Bacteriology*, 170(3):1046–1053, 1988.

[23] N.K. Gaur, E. Dubnau, and I. Smith. Characterization of a cloned *Bacillus subtilis* gene that inhibits sporulation in multiple copies. *Journal of Bacteriology*, 168(2):860–869, 1986.

[24] N.K. Gaur, J. Oppenheim, and I. Smith. The *Bacillus subtilis sin* gene, a regulator of alternate developmental processes, codes for a DNA-binding protein. *Journal of Bacteriology*, 173(2):678–686, 1991.

[25] L. Glass and S.A. Kauffman. The logical analysis of continuous non-linear biochemical control networks. *Journal of Theoretical Biology*, 39:103–129, 1973.

[26] J.-L. Gouzé and T. Sari. A class of piecewise linear differential equations arising in biological models. Technical Report RR-4207, INRIA, Sophia-Antipolis, 2001.

[27] C.E. Grimshaw, S. Huang, C.G. Hanstein, M.A. Strauch, D. Burbulys, L. Wang, J.A. Hoch, and J.M. Whiteley. Synergistic kinetic interactions between components of the phosphorelay controlling sporulation in *Bacillus subtilis*. *Biochemistry*, 37:1365–1375, 1998.

[28] A.D. Grossman. Genetic networks controlling the initiation of sporulation and the development of genetic competence in *Bacillus subtilis*. *Annual Review of Genetics*, 29:477–508, 1995.

[29] J.F. Guespin-Michel. Phenotypic reversion in some early blocked sporulation mutants of *Bacillus subtilis*: Isolation and phenotype identification of partial revertants. *Journal of Bacteriology*, 108(1):241–247, 1971.

[30] W.G. Haldenwang. The sigma factors of *Bacillus subtilis*. *Microbiological Reviews*, 59(1):1–30, 1995.

[31] J. Healy, J. Weir, I. Smith, and R. Losick. Post-transcriptional control of a sporulation regulatory gene encoding transcription factor σ^H in *Bacillus subtilis*. *Molecular Microbiology*, 5(2):477–487, 1991.

[32] M. Hecker and U. Völker. General stress response of *Bacillus subtilis* and other bacteria. *Advances in Microbial Physiology*, 44:35–91, 2001.

[33] R. Heinrich and S. Schuster. *The Regulation of Cellular Systems*. Chapman & Hall, New York, 1996.

[34] J.A. Hoch. Genetics of bacterial sporulation. *Advances in Genetics*, 18:69–98, 1976.

[35] J.A. Hoch. Regulation of the phosphorelay and the initiation of sporulation in *Bacillus subtilis*. *Annual Review of Microbiology*, 47:441–465, 1993.

[36] K.J. Jaacks, J. Healy, R. Losick, and A.D. Grossman. Identification and characterization of genes controlled by the sporulation-regulatory gene *spo0H* in *Bacillus subtilis*. *Journal of Bacteriology*, 171(8):4121–4129, 1989.

[37] M. Jiang, W. Shao, M. Perego, and J.A. Hoch. Multiple histidine kinases regulate entry into stationary phase and sporulation in *Bacillus subtilis*. *Molecular Microbiology*, 38(3):535–542, 2000.

[38] P.T. Kallio, J.E. Fagelson, J.A. Hoch, and M.A. Strauch. The transition state regulator Hpr of *Bacillus subtilis* is a DNA-binding protein. *Journal of Biological Chemistry*, 266(20):13411–13417, 1991.

[39] S.A. Kauffman. *The Origins of Order: Self-Organization and Selection in Evolution*. Oxford University Press, New York, 1993.

[40] A.D. Keller. Model genetic circuits encoding autoregulatory transcription factors. *Journal of Theoretical Biology*, 172:169–185, 1995.

[41] K. Kobayashi, K. Shoji, T. Shimizu, K. Nakano, T. Sato, and Y. Kobayashi. Analysis of a suppressor mutation *ssb* (*kinC*) of *sur0B20* (*spo0A*) mutation in *Bacillus subtilis* reveals that *kinC* encodes a histidine protein kinase. *Journal of Bacteriology*, 177(1):176–182, 1995.

[42] K.W. Kohn. Molecular interaction maps as information organizers and simulation guides. *Chaos*, 11(1):1–14, 2001.

[43] L. Kroos, B. Zhang, H. Ichikawa, and Y.-T. N. Yu. Control of σ factor activity during *Bacillus subtilis* sporulation. *Molecular Microbiology*, 31(5):1285–1294, 1999.

[44] J. Kudoh, T. Ikeuchi, and K. Kurahashi. Nucleotide sequences of the sporulation gene *spo0A* and its mutant genes of *Bacillus subtilis*. *Proceedings of the National Academy of Sciences of the USA*, 82(9):2665–2668, 1985.

[45] B.A. Lazazzera, I.G. Kurtser, R.S. McQuade, and A.D. Grossman. An autoregulatory circuit affecting peptide signaling in *Bacillus subtilis*. *Journal of Bacteriology*, 181(17):5193–5200, 1999.

[46] J.R. LeDeaux and A.D. Grossman. Isolation and characterization of *kinC*, a gene that encodes a sensor kinase homologous to the sporulation sensor kinases KinA and KinB in *Bacillus subtilis*. *Journal of Bacteriology*, 177(1):166–175, 1995.

[47] J.R. LeDeaux, N. Yu, and A.D. Grossman. Different roles for KinA, KinB, and KinC in the initiation of sporulation in *Bacillus subtilis*. *Journal of Bacteriology*, 177(3):861–863, 1995.

[48] P.A. Levin and A.D. Grossman. Cell cycle and sporulation in *Bacillus subtilis*. *Current Opinion in Microbiology*, 1(6):630–635, 1998.

[49] R.J. Lewis, D.J. Scott, J.A. Brannigan, J.C. Ladds, M.A. Cervin, G.B. Spiegelman, J.G. Hoggett, I. Barak, and A.J. Wilkinson. Dimer formation and transcription activation in the sporulation response regulator Spo0A. *Journal of Molecular Biology*, 316(2):235–245, 2002.

[50] P. Louie, A. Lee, K. Stansmore, R. Grant, C. Ginther, and T. Leighton. Roles of *rpoD*, *spoIIF*, *spoIIJ*, *spoIIN*, and *sin* in regulation of *Bacillus subtilis* stage II sporulation-specific transcription. *Journal of Bacteriology*, 174(11):3570–3576, 1992.

[51] I. Mandić-Mulec, N. Gaur, U. Bai, and I. Smith. Sin, a stage-specific repressor of cellular differentiation. *Journal of Bacteriology*, 174(11):3561–3569, 1992.

[52] I. Mandić-Mulic, L. Doukhan, and I. Smith. The *Bacillus subtilis* SinR protein is a repressor of the key sporulation gene *spo0A*. *Journal of Bacteriology*, 177(16):4619–4627, 1995.

[53] L. Mendoza, D. Thieffry, and E.R. Alvarez-Buylla. Genetic control of flower morphogenesis in *Arabidopsis thaliana*: A logical analysis. *Bioinformatics*, 15(7-8):593–606, 1999.

[54] T. Mestl, E. Plahte, and S.W. Omholt. A mathematical framework for describing and analysing gene regulatory networks. *Journal of Theoretical Biology*, 176:291–300, 1995.

[55] I. Moszer, P. Glaser, and A. Danchin. SubtiList: A relational database for the *Bacillus subtilis* genome. *Microbiology*, 141:261–268, 1995.

[56] J.P. Mueller, G. Bukusoglu, and A.L. Sonenshein. Transcriptional regulation of *Bacillus subtilis* glucose starvation-inducible genes: control of *gsiA* by the ComP-ComA signal transduction system. *Journal of Bacteriology*, 174(13):4361–4373, 1992.

[57] M. Perego. Kinase-phosphatase competition regulates *Bacillus subtilis* development. *Trends in Microbiology*, 6(9):366–370, 1998.

[58] M. Perego, S.P. Cole, D. Burbulys, K. Trach, and J.A. Hoch. Characterization of the gene for a protein kinase which phosphorylates the sporulation-regulatory proteins Spo0A and Spo0F of *Bacillus subtilis*. *Journal of Bacteriology*, 171(11):6187–6196, 1989.

[59] M. Perego and J.A. Hoch. Isolation and sequence of the *spo0E* gene: its role in initiation of sporulation in *Bacillus subtilis*. *Molecular Microbiology*, 1(1):125–132, 1987.

[60] M. Perego and J.A. Hoch. Sequence analysis of the *hpr* locus, a regulatory gene for protease production and sporulation in *Bacillus subtilis*. *Journal of Bacteriology*, 170(6):2560–2567, 1988.

[61] M. Perego and J.A. Hoch. Negative regulation of *Bacillus subtilis* sporulation by the *spo0E* gene product. *Journal of Bacteriology*, 173(8):2514–2520, 1991.

[62] M. Perego, G.B. Spiegelman, and J.A. Hoch. Structure of the gene for the transition state regulator, *abrB*: Regulator synthesis is controlled by the *spo0A* sporulation gene in *Bacillus subtilis*. *Molecular Microbiology*, 2(6):689–699, 1988.

[63] M. Perego, J.J. Wu, G.B. Spiegelman, and J.A. Hoch. Mutational dissociation of the positive and negative regulatory properties of the Spo0A sporulation transcription factor of *Bacillus subtilis*. *Gene*, 100:207–212, 1991.

[64] Z.E. Phillips and M.A. Strauch. *Bacillus subtilis* sporulation and stationary phase gene expression. *Cellular and Molecular Life Sciences*, 59(3):392–402, 2002.

[65] M. Predich, G. Nair, and I. Smith. *Bacillus subtilis* early sporulation genes *kinA*, *spo0F*, and *spo0A* are transcribed by the RNA polymerase containing σ^H. *Journal of Bacteriology*, 174(9):2771–2778, 1992.

[66] M. Ptashne. *A Genetic Switch: Phage λ and Higher Organisms*. Cell Press & Blackwell Science, Cambridge, MA, 2nd edition, 1992.

[67] L. Sánchez and D. Thieffry. A logical analysis of the *Drosophila* gap genes. *Journal of Theoretical Biology*, 211:115–141, 2001.

[68] L.A. Segel. *Modeling Dynamic Phenomena in Molecular and Cellular Biology*. Cambridge University Press, Cambridge, 1984.

[69] E. Shacter, P.B. Chock, and E.R. Stadtman. Regulation through phosphorylation/dephosphorylation cascade systems. *Journal of Biological Chemistry*, 259(19):12252–12259, 1984.

[70] S.H. Shafikhani, I. Mandic-Mulec, M.A. Strauch, I. Smith, and T. Leighton. Postexponential regulation of *sin* operon expression in *Bacillus subtilis*. *Journal of Bacteriology*, 184(2):564–571, 2002.

[71] K.J. Siranosian and A.D. Grossman. Activation of *spo0A* transcription by σ^H is necessary for sporulation but not for competence in *Bacillus subtilis*. *Journal of Bacteriology*, 176(12):3812–3815, 1994.

[72] I. Smith. Regulatory proteins that control late-growth development. In A.L. Sonenshein, J.A. Hoch, and R. Losick, editors, *Bacillus subtilis and other Gram-Positive Bacteria: Biochemistry, Physiology, and Molecular Genetics*, pages 785–800. American Society for Microbiology, Washington, DC, 1993.

[73] I. Smith, I. Mandić-Mulec, and N. Gaur. The role of negative control in sporulation. *Research in Microbiology*, 142:831–839, 1991.

[74] E.H. Snoussi. Qualitative dynamics of piecewise-linear differential equations: A discrete mapping approach. *Dynamics and Stability of Systems*, 4(3-4):189–207, 1989.

[75] A.L. Sonenshein. Bacterial sporulaton: A response to environmental signals. In G. Storz and R. Hengge-Aronis, editors, *Bacterial Stress Responses*, chapter 13, pages 199–215. American Society for Microbiology, Washington, DC, 2000.

[76] A.L. Sonenshein. Control of sporulation initiation in *Bacillus subtilis*. *Current Opinion in Microbiology*, 3:561–566, 2000.

[77] P. Stragier and R. Losick. Molecular genetics of sporulation in *Bacillus subtilis*. *Annual Review of Genetics*, 30:297–341, 1996.

[78] M.A. Strauch. AbrB, a transition state regulator. In A.L. Sonenshein, J.A. Hoch, and R. Losick, editors, *Bacillus subtilis and other Gram-Positive Bacteria: Biochemistry, Physiology, and Molecular Genetics*, pages 757–764. American Society for Microbiology, Washington, DC, 1993.

[79] M.A. Strauch. Regulation of *Bacillus subtilis* gene expression during the transition from exponential growth to stationary phase. *Progress in Nucleic Acid Research and Molecular Biology*, 46:121–153, 1993.

[80] M.A. Strauch and J.A. Hoch. Transition-state regulators: Sentinels of *Bacillus subtilis* post-exponential gene expression. *Molecular Microbiology*, 7(3):337–342, 1993.

[81] M.A. Strauch, G.B. Spiegelman M. Perego, W.C. Johnson, D. Burbulys, and J.A. Hoch. The transition state transcription regulator *abrB* of *Bacillus subtilis* is a DNA binding protein. *EMBO Journal*, 8(5):1615–1621, 1989.

[82] M.A. Strauch, M. Perego, D. Burbulys, and J.A. Hoch. The transition state transcription regulator AbrB of *Bacillus subtilis* is autoregulated during vegetative growth. *Molecular Microbiology*, 3(9):1203–1209, 1989.

[83] M.A. Strauch, K.A. Trach, J. Day, and J.A. Hoch. Spo0A activates and represses its own synthesis by binding at its dual promoters. *Biochimie*, 74:619–626, 1992.

[84] D. Thieffry and R. Thomas. Dynamical behaviour of biological networks: II. Immunity control in bacteriophage lambda. *Bulletin of Mathematical Biology*, 57(2):277–297, 1995.

[85] R. Thomas and R. d'Ari. *Biological Feedback*. CRC Press, Boca Raton, FL, 1990.

[86] K. Trach, D. Burbulys, M. Strauch, J.-J. Wu, N. Dhillon, R. Jonas, C. Hanstein, P. Kallio, M. Perego, T. Bird, G. Spiegelman, C. Fogher, and J.A. Hoch. Control of the initiation of sporulation in *Bacillus subtilis* by a phosphorelay. *Research in Microbiology*, 142:815–823, 1991.

[87] K.A. Trach and J.A. Hoch. Multisensory activation of the phosphorelay initiating sporulation in *Bacillus subtilis*: Identification and sequence of the protein kinase of the alternate pathway. *Molecular Microbiology*, 8(1):69–79, 1993.

[88] J.L. Vaughn, V. Feher, S. Naylor, M.A. Strauch, and J. Cavanagh. Novel DNA binding domain and genetic regulation model of *Bacillus subtilis* transition state regulator *abrB*. *Nature Structural Biology*, 7(12):1139–1146, 2000.

[89] L. Wang, R. Grau, M. Perego, and J.A. Hoch. A novel histidine kinase inhibitor regulating development in *Bacillus subtilis*. *Genes & Development*, 11:2569–2579, 1997.

[90] J. Weir, E. Dubnau, N. Ramakrishna, and I. Smith. *Bacillus subtilis spo0H* gene. *Journal of Bacteriology*, 157(2):405–412, 1984.

[91] J. Weir, M. Predich, E. Dubnau, G. Nair, and I. Smith. Regulation of *spo0H*, a gene coding for the *Bacillus subtilis* σ^H factor. *Journal of Bacteriology*, 173(2):521–529, 1991.

[92] D.M. Wolf and F.H. Eeckman. On the relationship between genomic regulatory element organization and gene regulatory dynamics. *Journal of Theoretical Biology*, 195:167–186, 1998.

[93] J.-J. Wu, M.G. Howard, and P.J. Piggot. Regulation of transcription of the *Bacillus subtilis spoIIA locus*. *Journal of Bacteriology*, 171(2):692–698, 1989.

[94] J.-J. Wu, P.J. Piggot, K.M. Tatti, and C.P. Moran, Jr. Transcription of the *Bacillus subtilis spoIIA* locus. *Gene*, 101:113–116, 1991.

[95] G. Yagil and E. Yagil. On the relation between effector concentration and the rate of induced enzyme synthesis. *Biophysical Journal*, 11:11–27, 1971.

[96] S. Yamashita, F. Kawamura, H. Yoshikawa, H. Takahashi, Y. Kobayashi, and H. Saito. Dissection of the expression signals of the *spo0A* gene of the *Bacillus subtilis*: Glucose represses sporulation-specific expression. *Journal of General Microbiology*, 135:1335–1345, 1989.

Unité de recherche INRIA Rhône-Alpes
655, avenue de l'Europe - 38330 Montbonnot-St-Martin (France)

Unité de recherche INRIA Lorraine : LORIA, Technopôle de Nancy-Brabois - Campus scientifique
615, rue du Jardin Botanique - BP 101 - 54602 Villers-lès-Nancy Cedex (France)
Unité de recherche INRIA Rennes : IRISA, Campus universitaire de Beaulieu - 35042 Rennes Cedex (France)
Unité de recherche INRIA Rocquencourt : Domaine de Voluceau - Rocquencourt - BP 105 - 78153 Le Chesnay Cedex (France)
Unité de recherche INRIA Sophia Antipolis : 2004, route des Lucioles - BP 93 - 06902 Sophia Antipolis Cedex (France)

Éditeur
INRIA - Domaine de Voluceau - Rocquencourt, BP 105 - 78153 Le Chesnay Cedex (France)
http://www.inria.fr
ISSN 0249-6399